

National Library
of Canada

Canadian Theses Service

Ottawa, Canada
K1A 0N4

Bibliothèque nationale
du Canada

Services des thèses canadiennes

CANADIAN THESES

THÈSES CANADIENNES

NOTICE

The quality of this microfiche is heavily dependent upon the quality of the original thesis submitted for microfilming. Every effort has been made to ensure the highest quality of reproduction possible.

If pages are missing, contact the university which granted the degree.

Some pages may have indistinct print especially if the original pages were typed with a poor typewriter ribbon or if the university sent us an inferior photocopy.

Previously copyrighted materials (journal articles, published tests, etc.) are not filmed.

Reproduction, in full or in part of this film is governed by the Canadian Copyright Act, R.S.C. 1970, c. C-30.

AVIS

La qualité de cette microfiche dépend grandement de la qualité de la thèse soumise au microfilmage. Nous avons tout fait pour assurer une qualité supérieure de reproduction.

S'il manque des pages, veuillez communiquer avec l'université qui a conféré le grade.

La qualité d'impression de certaines pages peut laisser à désirer, surtout si les pages originales ont été dactylographiées à l'aide d'un ruban usé ou si l'université nous a fait parvenir une photocopie de qualité inférieure.

Les documents qui sont déjà l'objet d'un droit d'auteur (articles de revue, examens publiés, etc.) ne sont pas microfilmés.

La reproduction, même partielle, de ce microfilm est soumise à la Loi canadienne sur le droit d'auteur, SRC 1970, c. C-30.

THIS DISSERTATION
HAS BEEN MICROFILMED
EXACTLY AS RECEIVED

LA THÈSE A ÉTÉ
MICROFILMÉE TELLE QUE
NOUS L'AVONS REÇUE

A Plastic Scintillator As A Probe For A Portable
Survey Meter

M. Nurul Mustafa

A Thesis
in
The Department
of
Physics

Presented in Partial Fulfillment of the Requirements
for the Degree of Master of Science at
Concordia University
Montréal, Québec, Canada

August 1986

© M. Nurul Mustafa, 1986

Permission has been granted
to the National Library of
Canada, to microfilm this
thesis and to lend or sell
copies of the film.

The author (copyright owner)
has reserved other
publication rights, and
neither the thesis nor
extensive extracts from it
may be printed or otherwise
reproduced without his/her
written permission.

L'autorisation a été accordée
à la Bibliothèque nationale
du Canada de microfilmer
cette thèse et de prêter ou
de vendre des exemplaires du
film.

L'auteur (titulaire du droit
d'auteur) se réserve les
autres droits de publication;
ni la thèse ni de longs
extraits de celle-ci ne
doivent être imprimés ou
autrement reproduits sans son
autorisation écrite.

ISBN 0-315-32245-4

ABSTRACT

A Plastic Scintillator As A Probe For A Portable Survey Meter.

M. Nurul Mustafa

To use a plastic scintillator to estimate the absorbed dose in a portable survey meter, a Monte Carlo computer code has been developed in FORTRAN 77. The response of NE102A plastic scintillator relative to muscle has been studied at various photon energies. Good agreement was obtained between the experimental spectra and Monte Carlo spectra. The calibration of the detector was done by comparing the experimental and Monte Carlo spectra.

The total energy absorbed in the plastic scintillator and total energy incident on the scintillator was found essentially to be independent of incident photon energy.

The background radiation was measured with a plastic scintillator for three months. The results are in good agreement with the published values of Hanson and Komarov.²⁰

ACKNOWLEDGEMENTS

The author expresses his deep gratitude to Dr.D.E.Charlton and Dr.N.W.Eddy for their active guidance, help and advice to complete this work.

The author is grateful to Professor S.K.Misra for his advice, help and encouragement.

The author would like to thank Professor C.S.Kalman for his encouragement and help.

The author is grateful to the Concordia University Graduate Fellowship Committee for awarding him the Concordia University Graduate Fellowship. He gratefully acknowledges the teaching assistantship received from the Physics Department.

Lastly, but not the least, the author wishes to extend his appreciation to his wife Zahan, daughter Aunu and son Asif who are far from him for three years. Their sacrifices and continued encouragement will never be forgotten.

TABLE OF CONTENTS

| | |
|--|------|
| ABSTRACT | iii |
| ACKNOWLEDGEMENTS | iv |
| LIST OF FIGURES | viii |
| LIST OF TABLES | x |
| CHAPTER 1 INTRODUCTION | 1 |
| 1.1 Usefulness of scintillation detection for dosimetry | 4 |
| CHAPTER 2 THE INTERACTION OF RADIATION WITH MATTER | 6 |
| 2.1 Photoelectric effect | 7 |
| 2.2 The Compton effect | 9 |
| 2.3 Pair production | 14 |
| 2.4 Attenuation law | 16 |
| 2.5 The mass-energy transfer coefficient | 19 |
| 2.6 The mass-energy absorption coefficient | 20 |
| CHAPTER 3 MONTE CARLO METHOD | 22 |
| 3.1 Random number generation | 23 |
| 3.2 The method of forcing interaction of photon inside the detector | 24 |
| 3.3 Decision processes | 26 |
| 3.4 Co-ordinates of photon in the scintillator | 27 |
| 3.5 Photoelectric process | 32 |
| 3.6 Compton process | 33 |
| 3.7 Pair production | 34 |
| 3.8 Smearing of spectrum | 35 |

| | | |
|------------------|--|-----------|
| CHAPTER 4 | CALCULATION OF DOSE | 45 |
| 4.1 | Exposure | 45 |
| 4.2 | Exposure rate | 45 |
| 4.3 | Absorbed dose | 46 |
| 4.4 | Absorbed dose rate | 47 |
| 4.5 | Calculation of absorbed dose from gamma radiation | 47 |
| 4.6 | Relation between gamma flux density and exposure rate | 48 |
| 4.7 | Specific gamma ray constant (Γ) | 50 |
| 4.8 | The energy absorbed in plastic scintillator is independent of incident photon energy | 51 |
| 4.9 | Response of plastic scintillator relative to muscle | 55 |
| 4.10 | Accuracy of Monte Carlo program | 63 |
| CHAPTER 5 | EXPERIMENTAL TECHNIQUE | 65 |
| 5.1 | Detection assembly | 65 |
| 5.2 | Amplification system | 67 |
| 5.3 | Data accumulation | 67 |
| 5.4 | Linearity of detection system | 68 |
| 5.5 | Spectrum transfer | 68 |

| | | |
|------------|---|----|
| 5.6 | Calibration of detector | 70 |
| 5.7 | Dose determination with a plastic scintillator | 71 |
| CHAPTER 6 | BACKGROUND RADIATION | 79 |
| CHAPTER 7 | DISCUSSIONS | 83 |
| REFERENCES | | 88 |
| APPENDIX | Listing of computer programs | 91 |

LIST OF FIGURES

| | |
|---|----|
| 2.1 Schematic representation of photoelectric effect | 8 |
| 2.2 Schematic representation of the Compton effect | 11 |
| 2.3 Schematic representation of pair production | 15 |
| 2.4 The cross sections of NE102A for each of the three types of interactions as a function of energy | 17 |
| 3.1 Co-ordinates of photon in the detector | 29 |
| 3.2 Monte Carlo spectrum for ^{137}Cs | 37 |
| 3.3 Smeared Monte Carlo spectrum for ^{137}Cs | 38 |
| 3.4 Monte Carlo spectrum for ^{60}Co | 39 |
| 3.5 Smeared Monte Carlo spectrum for ^{60}Co | 40 |
| 4.1 The value of K as a function of incident energies | 54 |
| 4.2 Response of plastic scintillator relative to muscle | |
| (a) Plot of $(\mu \text{ en}^{\beta})_{\text{plastic}} / (\mu \text{ en}^{\beta})_{\text{muscle}}$ as a function of energy | 59 |
| (b) Plot of the ratio between the energy absorbed in plastic and muscle calculated by Monte Carlo method, as a function of energy | 61 |
| 5.1 Block diagram of experimental setup | 66 |
| 5.2 Linearity of detection system | 69 |
| 5.3 Experimental spectrum for ^{137}Cs | 73 |
| 5.4 Experimental and smeared Monte Carlo spectra for ^{137}Cs | 74 |

| | | |
|-----|---|----|
| 5.5 | Experimental spectrum for ^{60}Co | 75 |
| 5.6 | Experimental and smeared Monte Carlo spectra for ^{60}Co | 76 |
| 5.7 | Calibration curve of plastic detector (using mid-point of spectra) | 77 |
| 5.8 | Calibration curve of plastic detector (using half height of spectra) | 78 |
| 6.1 | A typical background spectrum | 80 |
| 6.2 | Daily variation of background radiation | 82 |

LIST OF TABLES

| | | |
|-----|---|----|
| 3.1 | Cross sections of Hydrogen | 41 |
| 3.2 | Cross sections of Carbon | 42 |
| 3.3 | Cross sections of NE102A plastic scintillator | 43 |
| 3.4 | Cross sections of muscle | 44 |
| 4.1 | Value of K for various incident energies | 53 |
| 4.2 | Mass energy absorption coefficients (μ_{en}/ρ) of H, C, O and N | 57 |
| 4.3 | Mass energy absorption coefficients of NE102A and muscle | 58 |
| 4.4 | Response of NE102A relative to muscle | 62 |
| 4.5 | Gamma dose/photon calculated from Monte Carlo method and specific gamma ray constant (Γ) | 64 |

CHAPTER 1

INTRODUCTION.

It is well known that all living things are exposed to radiations from natural background and man-made radionuclides. With increasing use of artificial radionuclides and nuclear power reactors etc, there is a possible change in the environmental levels of radioactivity. This has become a cause for concern, so there has been increasing interest in accurately measuring the levels of radioactivity in man and his environment.

Many types of scintillator counters have been devised and used for radiation measurement. They are capable of great sensitivity and high count rates and can measure absorbed dose, exposure or fluence if calibrated for energy range of interest. For each photon or particle detected, a single pulse is usually counted but the size of this pulse is related to the energy deposited in the scintillator. Hence a measurement can be obtained of the energy absorbed in the scintillator.

The aim of this work is to examine a solid detecting material in which the average rate of energy deposition, that is absorbed dose rate, would match as closely as possible with soft tissue (muscle). A low atomic number (2) material resembling the atomic number of human tissue is desirable, so NE102A plastic scintillator was chosen as the detector.

To use a plastic scintillator to estimate dose in a portable survey meter, it is necessary to determine the response of such a detector to a variety of radiations. There are many Monte Carlo calculations of response of NaI(Tl) and Ge(Li) detectors to gamma rays. There are several examples of these [NaI(Tl)^{1,2} and Ge(Li)³⁻⁵] but few for plastic scintillators such as References 6 and 7.

Because the photoelectric cross-section is so small in the low-Z material of plastic, the primary interaction is the Compton effect at low energies and pair production at higher energies. In calculation of dose, one requires only the total energy deposited per unit mass of absorbing material. One is less interested in details of the incident spectral distribution (such as photopeak centroid position), and more interested in the average effect on the detector material. The response of plastic scintillator up to 5 MeV is essentially due to the Compton scattering, hence it cannot be used for spectroscopic purposes which demands the detection of a sharp gamma line.

It will be shown that the proportionality factor between the absorbed energy in the plastic scintillator and the incident energy striking it is essentially independent of incident gamma ray energy. Thus a plastic scintillator can be used to measure the total energy absorbed in any environment. Its greater efficiency compared to gas detectors and its ruggedness should make it especially useful as a survey meter in low count rate situations.

To calculate energy spectra, a Monte Carlo computer code MONCA has been developed in FORTRAN 77 to obtain the response of a 2"x2" NE102A plastic scintillator. This program has also been used to calculate the energy spectra of muscle. The listing of the program MONCA is given in Appendix.

To obtain the dose response curve of plastic scintillator material relative to muscle, a program DOSE has been written. The listing of the program DOSE is given in Appendix.

The background radiation has been measured with NE102A plastic scintillator and its daily variation is shown. The program BKGRND calculates the dose in rad/h or Roentgen/h. The program listing is given in Appendix.

1.1 Usefulness of scintillation detectors for dosimetry.

The usefulness of scintillation detectors in the field of dosimetry for biologically oriented applications depends on the elementary process of light emission in a scintillator in relationship to the radiation induced processes in tissue. In any substance, excitation and ionization of the atoms or molecules are the principal results of the absorption of energetic radiations. Both ionization and excitation lead to electronic transitions that may be accompanied by the emission of light. In certain situations, it can be expected that this light emission constitutes as good a measure of the absorbed radiation energy as the ionization of the gas in an ionization chamber. Moreover, the similarity in density and atomic number between tissue and many luminescent substances is an added advantage compared with the gaseous detectors. The applicability of scintillation measurements for dosimetric purposes seems therefore promising. The use of ionization chambers to measure doses raises construction problems relating to particle types and dose rate to be measured. The finite drift mobility of the ions produced in the gas results in a rather slow response time, of order of milliseconds in most cases, which leads to an appreciable dead time, during which the detector may not respond to fresh incident radiation and a slow rise time in charge

collection pulses again limiting the rate of detection.

The solid detector is effectively about 1000 times bigger than a gas counter of the same physical size. The disadvantage of this is that pulse rate is correspondingly higher and pulse pile-up and sorting can be a problem. This problem may be alleviated by using a fast PHA system.

CHAPTER 2

THE INTERACTION OF γ -RADIATION WITH MATTER.

Gamma rays carry no charge, their main interaction is with the electrons or atomic electromagnetic field. The primary interactions of gamma rays with matter result in the production of energetic secondary charged particles, usually electrons, and it is these charged particles and their interaction with matter that account for the actual transfer of energy and consequently cause the biological and chemical effects.

In this chapter, we shall discuss three major types of interaction of gamma radiation with matter, attenuation law, mass energy transfer coefficient, and mass energy absorption coefficient. These will be required in the following chapter when the photon transport code will be discussed in detail. The three major processes are;

1. Photoelectric process
2. Compton or incoherent process
3. Pair production

2.1 Photoelectric effect.

In the photoelectric effect, the incident photon loses all its energy, with essentially all of it going to one of the orbital electrons, the photon disappears and an electron is ejected from the atom. The electron involved will be ejected from the atom with an energy equal to that of the photon, less the energy required to free the electron from its orbital position, shown in figure 2.1. The energy relation is given by the Einstein relation

$$E = h\nu - E_X$$

(2.1)

where E is the energy of the photoelectron, $h\nu$ the energy of the photon and E_X is the binding energy of the X-shell electron. The probability of this interaction is highest with K-shell electrons if the energy exceeds the K-shell binding energy. Photoelectric absorption is the most probable process at low photon energies.

After the photoelectron is ejected, the absorber atom will emit its characteristic X-rays i.e. Fluorescent radiation or Auger electron. In the case of a high atomic number absorber, E_X is large and the fluorescent radiation is quite penetrating. Tissue on the other hand is for the most part composed of low Z-elements and E_X is less than 1 keV.

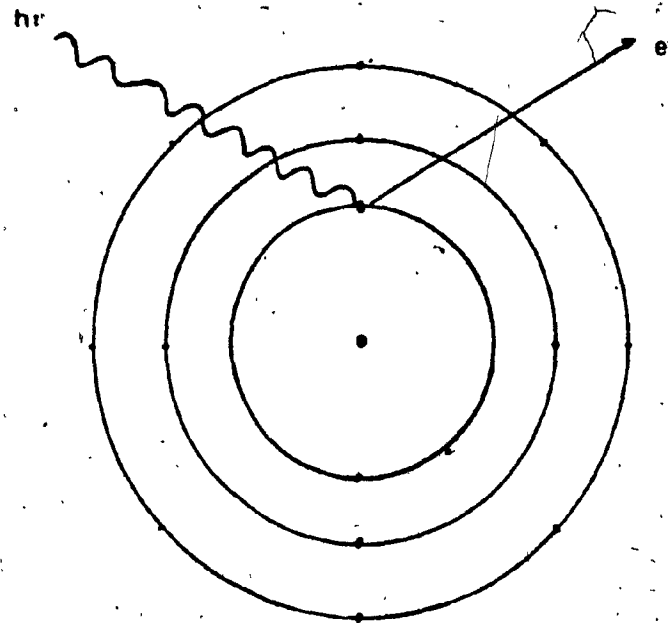


Figure 2.1 Schematic representation of photoelectric effect.

In this case the very soft fluorescent radiation will be absorbed very close to the point of emission and true transfer is the same as the incident photon energy. The fact that E_K is so small makes the distinction of little practical importance.

The photoelectric cross sections are strong functions of both energies of photon and atomic numbers of absorbing materials. They vary over a considerable range, approximately as

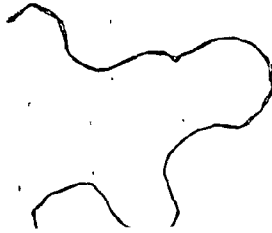
$$\tau = \text{const. } z^4 (h\nu)^{-3} \quad \text{cm}^2/\text{atom}$$

(2.2)

The general trend is a rapid increase in τ with atomic number and a rapid decrease as photon energy increases. Figure 2.4 shows the τ values for the plastic scintillator as a function of photon energies.

2.2 The Compton effect.

The Compton effect involves the interactions of a photon with a free electron at rest, and is quantified by the Klein-Nishina formula for differential cross section⁸. The Klein-Nishina theory applies when the incident photon energy is large compared with the binding energy of the electron. The interaction may be treated as an elastic collision between a photon (energy $h\nu$ and momentum $(h\nu/c)$)



and an electron (rest energy). The photon is scattered through an angle θ with lower energy $h\nu'$ and momentum $(h\nu'/c)$. — The electron emerges at an angle ϕ with kinetic energy E_{ce} and momentum mv shown in figure 2.2.

Using conservation of momentum and energy, with the relativistic relationship for electron mass m and its kinetic energy E_{ce}

$$m = m_0 (1 - \beta^2)^{-\frac{1}{2}}$$

(2.3)

$$E_{ce} = (m - m_0)c^2 = m_0 c^2 ((1 - \beta^2)^{-\frac{1}{2}})$$

(2.4)

where m_0 = electron rest mass and $\beta = v/c$.

Then

$$pc = (E_{ce}^2 + 2m_0^2 c^2)^{\frac{1}{2}}$$

(2.5)

The conservation of energy is given by

$$h\nu = h\nu' + E_{ce}$$

(2.6)

The conservation laws give the energy relation of the Compton scattered photon.⁹

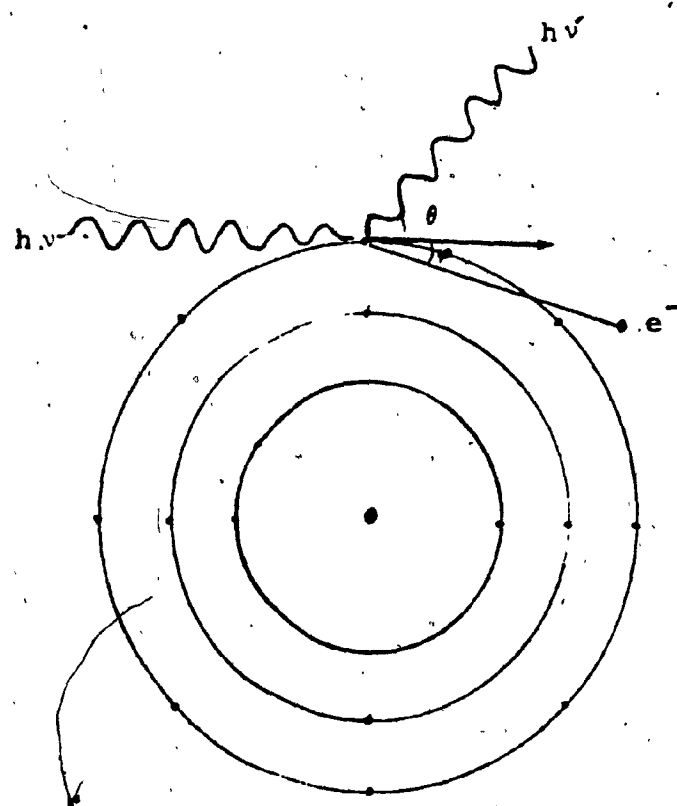


Figure 2.2 Schematic representation of the
Compton effect.

$$\bar{h\nu} = h\nu / \{1 + (h\nu/m_0 c^2)(1 - \cos\theta)\}$$

(2.7)

The energy imparted to the Compton electron is then

$$E_{ce} = h\nu - \bar{h\nu} = h\nu\alpha(1 - \cos\theta) / 1 + \alpha(1 - \cos\theta)$$

(2.8)

where $\alpha = h\nu/m_0 c^2$. The maximum value of E_{ce} corresponds to the minimum value of $\bar{h\nu}$, i.e. 180° scattering of photon. We have

$$E_{max} = h\nu / \{1 + 1/(2\alpha)\}$$

(2.9)

This energy denotes the "Compton edge", the maximum possible energy that the Compton electron can acquire in a single encounter. The Compton edge is the high energy end of the Compton recoil-electron energy distribution and is seen in the energy deposition spectrum in a scintillator as a broad peak below the energy of the incident gamma ray. The reason is that the energy distribution is broadened out somewhat by multiple Compton interaction and by the same type of inherent statistical fluctuations which produces the width of the total energy peak.⁹

The angle φ of the recoil Compton electron is related to the photon scattering angle θ , by

$$\cot \varphi = (1+\alpha) \tan \theta / 2$$

(2.10)

as θ goes from 0° to 180° , φ goes from 90° to 0°

The differential cross section per electron, for the number of photons scattered into a solid angle $d\Omega = 2\pi \sin \theta d\theta$, as derived theoretically by Klein-Nishina⁸ is

$$d\sigma/d\Omega = [r_0^2(1 + \cos^2 \theta)]/[2(1 + \alpha(1 - \cos \theta))^2] \{1 + [\alpha^2(1 - \cos \theta)^2]/[(1 + \cos^2 \theta)(1 + \alpha(1 - \cos \theta))]\}.$$

(2.11)

where $r_0 = 2.82 \times 10^{-13}$ cm, the classical electron radius.

The cross section σ is the probability of any Compton interaction by one photon while passing through a layer of material containing 1 electron/cm² is given by

$$\sigma = \int_0^\pi (d\sigma/d\Omega) 2\pi \sin \theta d\theta$$

(2.12)

$$= 2\pi r_0^2 ((1+\alpha)/\alpha^2) [2(1+\alpha)/(1+2\alpha) - (1/\alpha) \ln(1+2\alpha)] + \ln(1+2\alpha)/2\alpha - (1+3\alpha)/(1+2\alpha)^2 \text{ cm}^2/\text{electron}$$

(2.13)

The cross section for the atom is Z times the cross section per electron. Figure 2.4 shows the σ values for the plastic scintillator as a function of photon energies.

2.3 Pair production.

In the field of a charged particle (usually an atomic nucleus but also to some degree in the field of an atomic electron) a photon may be totally absorbed and an electron-positron pair is formed, as shown in figure 2.3. The photon energy appears as the total energy of the pair given as

$$h\nu = (E_- + m_0 c^2) + (E_+ + m_0 c^2)$$

(2.14)

A minimum incident photon energy of $h\nu = 2m_0 c^2$, is required for pair production in the field of a nucleus and a minimum of $h\nu = 4m_0 c^2$ in the field of an atomic electron. In a nuclear field, the kinetic energy of the electron-positron pair are distributed continuously, each from a minimum of zero up to a maximum of $(h\nu - 2m_0 c^2)$.

The energy spectra are essentially identical, and the electron's spectrum seldom matters as the interactions of electrons and positrons are almost similar and their ranges are small. The principal difference between

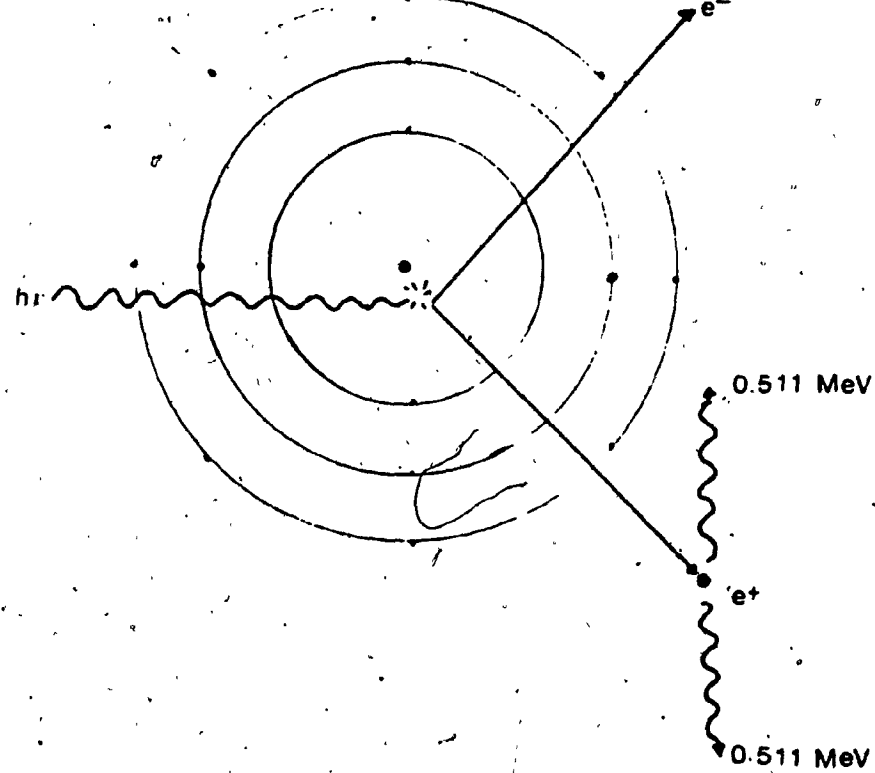


Figure 2.3 Schematic representation of pair production.

electrons and positrons is that the positron, on slowing down and combining with an electron, releases two annihilation photons of energy 0.511 MeV each, isotropically and in opposite directions. It is possible for these annihilation photons to travel some distance and they can be treated similar to Compton scattered photons in a Monte Carlo program.

The atomic cross section for nuclear pair production increases with Z^2 except above 5 MeV, where the cross section increases rapidly because the pair is created at some distance from the nucleus, and screening by the inner atomic electrons slightly reduces the effective Z. Also the cross section increases with the photon energy $h\nu$. Figure 2.4 shows the pair cross section κ for the plastic scintillator as a function of photon energies.

2.4. The attenuation law.

If we consider a beam of photons of intensity I_0 incident upon a plane of absorber, then at a depth x within the material this number has been reduced to I because of interactions with the absorber. Within an incremental distance dx at x there is a further reduction in I by an amount dI . The probability for interaction within dx is dI/I , and interaction per unit distance is $(dI/I).(1/dx)$. This latter probability has been given

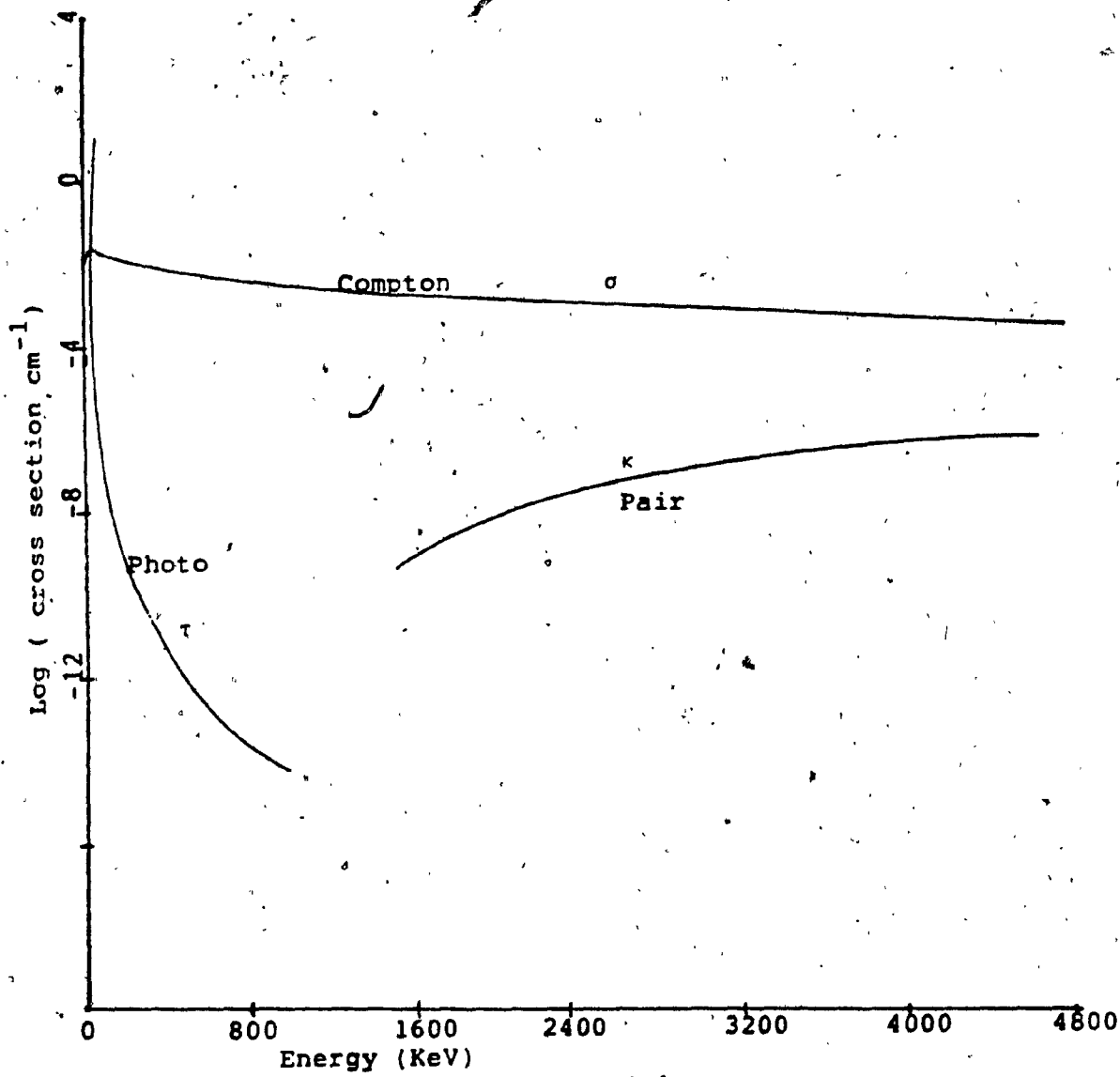


Figure 2.4 The cross sections of NE102A plastic scintillator for photoeffect, Compton scattering and pair production.

the name "linear attenuation coefficient" and is generally designated by the symbol μ with the dimensions of reciprocal centimeters (cm^{-1}). In terms of μ , we may write for the decrease in intensity within dx ,

$$-dI = \mu I dx$$

This differential equation, when solved by using boundary condition that $I=I_0$ at $x=0$, yields the familiar Lambert's law of exponential attenuation

$$I = I_0 \exp(-\mu x)$$

(2.15)

The cross sections or attenuation coefficients can also be expressed in units of barns/atom and cm^2/g . If the cross sections are expressed in barns/atom, it can be transformed into cm^{-1} when barns/atom is multiplied by the atomic density N , defined as¹⁰

$$N = N_A \rho / M \quad \text{atoms/cm}^3$$

(2.16)

where N_A is Avogadro's number, ρ is the density gm/cm^3 and M is atomic weight. The cross sections for photoelectric, Compton and pair production are usually denoted by τ , σ and κ respectively, then the total attenuation coefficient can be written as

$$\mu = (\tau + \sigma + \kappa) \quad \text{cm}^{-1}$$

(2.17)

and for the compound

$$\mu = \sum_i (\tau + \sigma + \kappa)_i \text{ cm}^{-1}$$

(2.18)

where Σ_i is the sum over the atoms of type i .

The attenuation coefficient is a measure of the number of primary photons undergoing interaction per unit distance in the target.

The mass attenuation coefficient is defined as

$$\mu/\rho = (\tau + \sigma + \kappa)/\rho \text{ cm}^2/\text{g.}$$

(2.19)

2.5 The mass-energy transfer coefficient, μ_K/ρ ¹¹

The mass energy transfer coefficient of a material for indirectly ionizing particles of specified energy is the quotient of dE_K/E by ρdl , where dE_K/E is the fraction of incident particle energy (excluding rest energy) that is transferred to the kinetic energy of charged particles by interaction in traversing a distance dl in a medium of density ρ .

$$\mu_K/\rho = dE_K/(\rho E dl)$$

(2.20)

For gamma photons of energy $h\nu$,

$$\mu_K/\rho = 1/\rho [\tau(1-\delta) + E/h\nu + \kappa(1 - 2m_0c^2/h\nu)] \quad (2.21)$$

where, τ =photoelectric cross section

δ =average energy emitted as fluorescent radiation
per absorbed photon

σ =total Compton cross section

E =average energy of the Compton electron

κ =pair production cross section

m_0c^2 =rest energy of electron

2.6 The mass-energy absorption coefficient, μ_{en}/ρ .¹¹

The mass energy absorption coefficient of a material for indirectly ionizing particles of specified energy is the product of mass energy transfer coefficient for that energy and $(1-G)$ where G is the fraction of energy lost by secondary charged particles in bremsstrahlung in that material. Bremsstrahlung losses due to slowing down of electrons and positrons in the detector material which become important only at higher energies (greater than 6 MeV) are neglected, and we assume here $G=0$, so

$$\mu_{en}/\rho = \mu_K/\rho$$

The mass energy absorption coefficient measures the amount of energy deposited in a medium by a photon interacting in medium. The absorption of energy is used in specifying radiation dose, and can be described in terms of mass energy absorption coefficient.

CHAPTER 3

MONTE CARLO METHOD

The principle of the Monte Carlo method consists of simulating the history of a large number of individual photons that pass through the scintillator. Each photon has its initial position coordinates, initial direction cosines and energy. The next step is to select 'path length', that is the distance to the first collision in units of mean free path. The selection is made with the aid of a random number. The routine will decide the types of interaction processes by using a random number with known probability distributions that are obtained from the cross sections of detector material. Only three types of interaction processes responsible for the energy deposition (the photoelectric effect, the Compton effect and pair production) are considered. The routine then computes the spatial coordinates of the collision point and direction cosines using the mean free path obtained from cross sections. The scattering angle is determined with the aid of random numbers, and scattered energy is computed . . . The program repeats until the photon is absorbed or escapes and then a new photon is considered.

In this chapter, the computer program MONCA is described in detail, in particular, descriptions are given of the method of forcing interactions of photons in the detector, determining types of photon interactions, coordinates of photon and energy deposition and other decision making processes. The "smearing out" of the initial spectrum from Monte Carlo calculation is also described.

3.1 Random number generation

Selection of path length, types of interaction, angle of scattering and many other parameters are made with the aid of a random number and these random numbers are often called pseudorandom. The sequence of pseudorandom numbers approximates the properties of true random numbers. Generally, a floating point number between 0 and 1 is desired because other distributions can be derived from this one.

By means of these pseudorandom numbers it is possible to obtain a random variable x from the probability distribution $p(x')$ from equation 3.1³

$$R = \int_{-\infty}^x p(x') dx' / \int_{-\infty}^{\infty} p(x') dx'$$

(3.1)

The right side of this equation may be tabulated for a number of x values so that it is possible to interpolate for each value of R .

All calculations have been done on a Cyber 170-835. The pseudo-random numbers uniformly distributed between 0 and 1 are obtained from the CDC library subroutine RANSET(n) which initializes the seed of the intrinsic function RANF() to generate random numbers. This random number is labeled by R .

3.2 The method of forcing interaction of photon inside the detector.

In order to collect good statistics, it is necessary to simulate the history of a large number of photons. Each photon uses computer time and it is important to minimize the computer processing time where possible. The photons which escape without interaction inside the detector will not deposit energy in the detector. Those photons are required to re-process in the program, thus increasing the computer processing time. A useful first step is to eliminate the photons which do not interact within the detector by the method of forcing all photons to interact inside the detector.

The point of interaction of the gamma photon in the detector volume is determined by sampling the exponential distribution of the gamma ray intensity. The intensity of gamma rays in the medium of total attenuation coefficient $\mu \text{ cm}^{-1}$ is distributed as a function of medium thickness according to Lambert's law,

$$I = I_0 \exp(-\mu r) \quad (3.2)$$

where I_0 is the intensity of gamma rays at the surface of detector and I that at a depth r into the medium. If R is a random number between 0 and 1 then by equation 3.1

$$R = \frac{\int_0^r I_0 \exp(-\mu r) dr}{\int_0^\infty I_0 \exp(-\mu r) dr}$$

Solving for r , we have

$$r = -\ln(1 - R)/\mu = -\ln(R)/\mu \quad (3.3)$$

since R is distributed in the same way as $(1-R)$.

If r smaller than the path available, that is thickness of the detector, then the photon is assumed to have undergone an interaction. On the other hand if r exceeds the detector thickness, the photon is presumed to have escaped without interaction. But we want each photon to interact at least once. The probability of making no interaction is $\exp(-\mu d)$, where d is detector thickness. The probability

of making at least one collision in the detector volume can be calculated for each photon by using the expression $(1 - \exp(-\mu d))$. This is equivalent to saying that if random numbers between 0 and $(1 - \exp(-\mu d))$ are drawn and used to calculate path length r then it will always be less than the thickness of the detector. Thus each photon is forced to interact at least once in the detector.

3.3 Decision processes.

Various steps in the history of the gamma ray before it escapes or is completely absorbed are simulated by applying random numbers modulated by known probability ratios or distributions. In the scintillator, only three possible interactions are considered, the photoelectric effect, Compton effect and pair production. The cross-sections for all three processes are obtained from Storm and Israel¹². The cross sections for these interactions in muscle are taken from J.H.Hubbell¹³. The cross sections for hydrogen and carbon in barns are given in table 3.1 and 3.2 which are used to calculate cross sections for NE102A. The cross sections in cm^2/g for NE102A and muscle are given in table 3.3 and 3.4 respectively. Since all cross sections and the attenuation coefficients were read into the computer in tabulated form, an interpolation procedure was used to calculate their values at any energy

point which does not coincide with the tabulated energy.

If we label the cross sections for the photoeffect, the Compton effect and pair production by τ , σ and κ respectively, then the probability for each type of interaction is given by τ/μ , σ/μ and κ/μ respectively, where μ is the sum of τ , σ , and κ . A random number will decide the type of interaction. If the random number R is in the interval between 0 and τ/μ then photoelectric process will follow and the program MONCA will call subroutine PHOTO. If R has the value between τ/μ and $(\tau + \kappa)/\mu$ pair production will occur and the program will call subroutine PAIR. If neither of these cases is selected, a Compton process results, and subroutine COMP will be called.

3.4 Co-ordinates of photon in the scintillator.

The path of gamma photon, its position of interaction and the energy loss at each interaction must be determined as the photon travels through the scintillator. After each interaction it needs to check whether the photon is inside the scintillator or has escaped.

Each interaction point of the gamma photon can be described by coordinates in the fixed system and the direction of motion by means of the direction cosines. After each interaction, the direction of motion of the photon and therefore its direction cosines are changed, so

it is necessary to recalculate the direction cosines after each event using the polar angle θ and azimuthal angle ϕ caused by an interaction.

Each gamma photon enters the scintillator along the z-axis, shown in figure 3.1. The initial position coordinates of the photon are

$$x_0 = 0$$

$$y_0 = 0$$

$$z_0 = 0$$

(3.4)

and the initial direction cosines are

$$\cos \alpha_0 = 0$$

$$\cos \beta_0 = 0$$

$$\cos \gamma_0 = 1$$

(3.5)

Each photon when entered into the detector is forced to interact at least once, as described in section 3.2.

The distance that the photon travels to the first interaction is calculated from the relation

$$r = -\ln R / \mu$$

(3.6)

where R is the random number and μ is the interpolated attenuation coefficient.

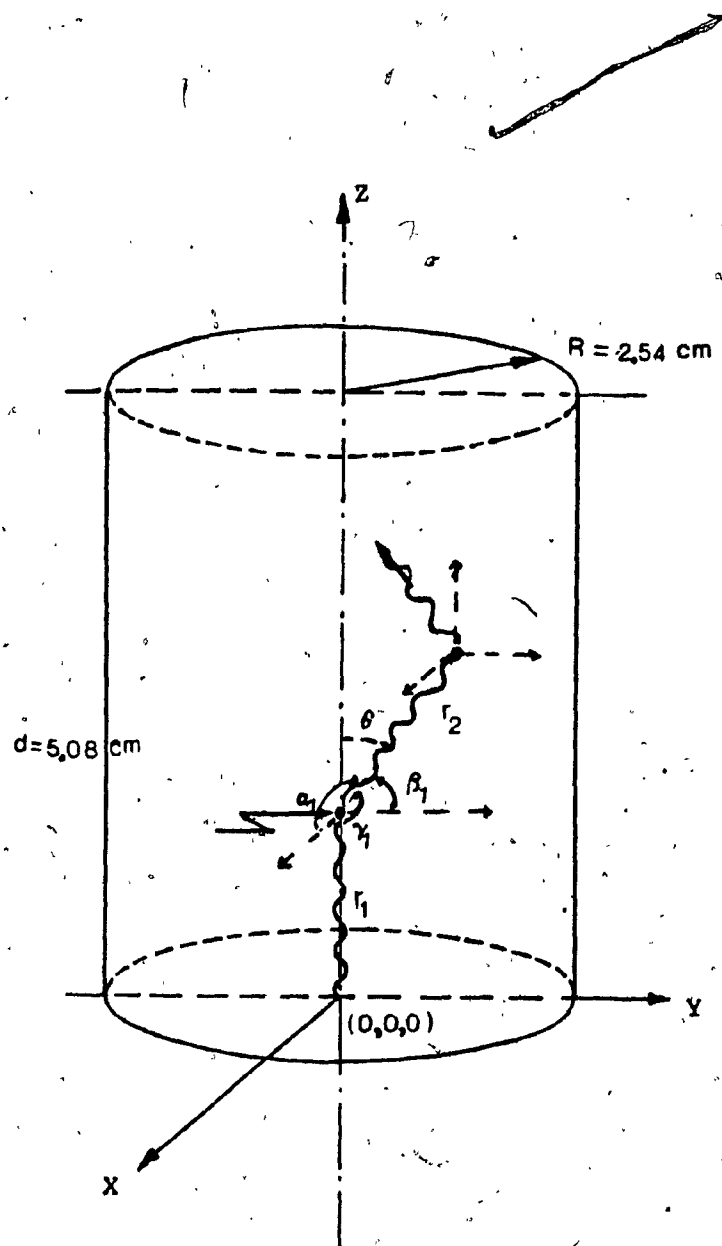


Figure 3.1 Schematic representation of photon co-ordinates in detector. The photon enters the detector along z -axis. A photon with position co-ordinates and directions $\cos\alpha, \cos\beta$ and $\cos\theta$ is shown. l is the path length and θ is polar angle.
 → shows the first interaction.

A new random number is drawn and type of interaction processes are determined as described in section 3.3. If the interaction is Compton then position coordinates and its direction cosines are calculated as described below, and the scattered photon and electron energies are calculated from the usual Compton relations, described in section 3.6.

The coordinates of the first interaction are then given by

$$x_1 = x_0 + r \cos \alpha_0$$

$$y_1 = y_0 + r \cos \beta_0$$

$$z_1 = z_0 + r \cos \gamma_0$$

(3.7)

The new set of direction cosines, with polar angle and azimuthal angle are to be calculated from equation (3.8) or (3.9) according to the condition that

when $|\cos \gamma_0| = 1$:

$$\cos \alpha_1 = \sin \theta \cos \varphi$$

$$\cos \beta_1 = \sin \theta \sin \varphi$$

$$\cos \gamma_1 = \cos \theta (\cos \gamma_0 / |\cos \gamma_0|)$$

(3.8)

and for $\cos\gamma_0 \neq 1$:

$$\begin{aligned}\cos\alpha_1 &= \cos\theta \cos\alpha_0 + ((1-\cos^2\theta)/(1-\cos^2\gamma_0))^{\frac{1}{2}} \\ &\quad (\cos\alpha_0 \cos\gamma_0 \cos\phi - \cos\beta_0 \sin\phi) \\ \cos\beta_1 &= \cos\theta \cos\beta_0 + ((1-\cos^2\theta)/(1-\cos^2\gamma_0))^{\frac{1}{2}} \\ &\quad (\cos\alpha_0 \cos\beta_0 \cos\phi + \cos\beta_0 \sin\phi) \\ \cos\gamma_1 &\neq \cos\theta \cos\gamma_0 - ((1-\cos^2\theta)/(1-\cos^2\gamma_0))^{\frac{1}{2}} \cos\phi(1-\cos^2\gamma_0)\end{aligned}$$

(3.9)

After the first interaction, the distance r' that the scattered photon travels can be calculated from equation (3.3) with a new random number and new attenuation coefficient, obtained by interpolation from the table of attenuation coefficients according to the scattered photon energy. The coordinates of the second interaction are then given by

$$x_2 = x_1 + r' \cos\alpha_1$$

$$y_2 = y_1 + r' \cos\beta_1$$

$$z_2 = z_1 + r' \cos\gamma_1$$

(3.10)

To check whether this interaction is inside the scintillator, we define

$$U = \left(\frac{x^2}{2} + \frac{y^2}{2} \right)^{\frac{1}{2}}$$

(3.11)

Now if U is greater than radius or z_2 greater than thickness or $z_2 \leq 0$ then the interaction is not inside the scintillator which means that photon has escaped. The energy deposited is stored and a new photon is considered. If the interaction is inside the scintillator, the process is repeated until the photon is absorbed or escapes. During the repetition process the energy deposited is summed. The equations (3.4 - 3.6) were used in the main program and equations (3.7 - 3.11) were used in the subroutine COMP.

3.5 Photo-electric process.

In the photoelectric effect the energy of the photoelectron is assumed to be equal to the incident photon energy neglecting the K-shell binding energy (E_K). For low Z-materials E_K is less than 1 keV. In this case the soft fluorescent radiation will be absorbed very close to the point of emission and true transfer is the same as the incident photon energy. The fact that E_K is so small makes the distinction of little practical importance. Thus $E = h\nu$.

The subroutine PHOTO was written with this assumption even though NE102A scintillator detector is composed.

of low Z-elements.

3.6 Compton process

The polar angle of the Compton scattered photon is determined by sampling the differential Klein-Nishina formula,

$$\frac{d\sigma}{d\Omega} = r_0^2 \frac{(1 + \cos^2\theta)}{[2(1 + E_0(1 - \cos\theta))^2]} \left\{ 1 + \frac{[E_0^2(1 - \cos\theta)^2] / [(1 + \cos^2\theta)(1 + E_0(1 - \cos\theta))]} \right\}$$

(3.12)

where $E_0 = E/m_0 c^2$, $r_0 = 2.82 \times 10^{-13}$ cm, the classical electron radius and m_0 is the electron rest mass. The polar angle θ which is distributed between 0° and 180° is determined from the relation (3.13), by equation (3.1) for random number,

$$F = \frac{\int_0^\theta (d\sigma/d\Omega) d\Omega}{\int_0^\pi (d\sigma/d\Omega) d\Omega}$$

(3.13)

To obtain the value of θ from the equation (3.13) the expression on the right side could be evaluated for various values of θ from 0° up to 180° . At each iteration the value is compared with the random number R until it is equal or just exceeds F which gives θ . This process of θ evaluation is time consuming. To save computer time, the expression

was evaluated for various values of θ in steps of 10^0 until $F \leq R$. The previous value of θ and current one then become lower and upper limits for a second scan, this time at 0.1^0 increments. This process of θ determination reduces computer processing time by about 80% without affecting the results. After determining the polar angle θ , the azimuthal angle ϕ of the Compton scattered photon is determined from a uniform distribution between 0 and 360^0 . The scattered photon energy is determined from the usual relation

$$E' = E / (1 + E_0(1 - \cos\theta))$$

(3.14)

The energy imparted to the Compton electron is then

$$E_{ce} = E - E'$$

(3.15)

We assumed this electron's energy is absorbed in the detector. The subroutine COMP was written using the above concepts and equations.

3.7 Pair production

For gamma rays of energies higher than $2m_0 c^2$, pair production becomes possible. In this process it is

assumed that the kinetic energy ($E - 2m_0c^2$) is shared equally by the electron-positron pair. Both positron and electron may cause ionization, hence energy is stored for each particle. When the annihilation of a positron occurs, two gamma photons of 0.511 MeV each are emitted. Each of these photons is treated again in the same manner as the Compton scattered photons.

The subroutine PAIR is written according to the above conditions.

3.8 Smearing of spectrum

To obtain a response spectrum, it is necessary to introduce line broadening into the initially determined spectrum derived from the Monte Carlo method. The line broadening is due to the variance in the collection of the optical photon produced in the scintillator and the statistical effects associated with the detection of these photons by the photomultiplier. The smearing out of the spectrum is obtained by application of a Gaussian resolution function using an experimentally determined resolution for comparing the response spectrum with the one obtained experimentally. A measure of the peak width is a quantity called the resolution of detector. It is defined as the full width at half maximum (denoted by F_w) of a given gamma ray peak divided by the peak energy E , times 100%. Thus if

R is resolution, then

$$R = (F_w / E) \cdot 100\%$$

(3.16)

If $C(n')$ represents the number of counts recorded in the n' th channel of spectrum obtained from Monte Carlo, then the distribution of counts in a new spectrum after applying a Gaussian resolution function is given by

$$F(n) = \{C(n')/\sigma\sqrt{2\pi}\} \exp(-{(n-n')^2}/2\sigma^2)$$

(3.17)

where $F(n)$ is the number of counts in the n th channel of smeared spectrum and

$$\sigma = F_w / 2.35482$$

(3.18)

$$\text{since FWHM} = F_w = 2\sqrt{2 \ln 2} \sigma$$

with F_w being experimentally determined full width at half maximum.

This smearing is done by the program 'SMEAR', its listing is given in the Appendix.

The initially determined Monte Carlo spectra and smeared spectra for ^{137}Cs and ^{60}Co are shown in figures 3.2, 3.3, 3.4, and 3.5 respectively.

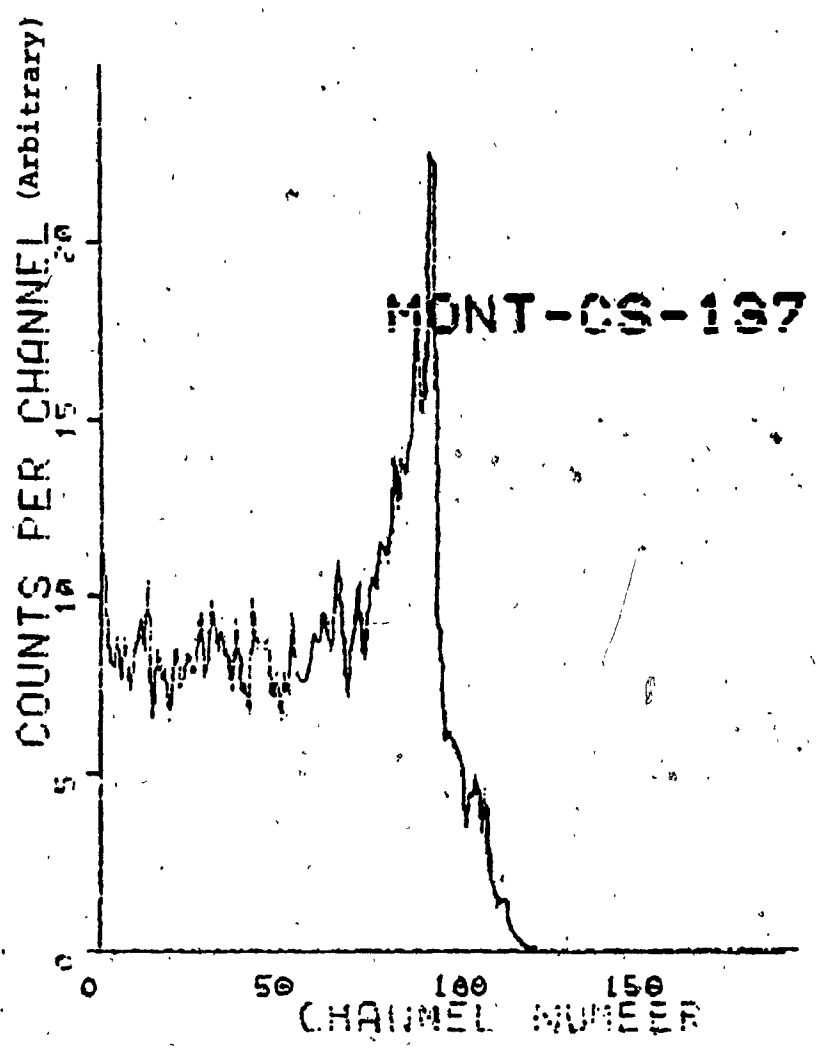


Figure 3.2 Monte Carlo spectrum for ^{137}Cs ,
one channel = 5 KeV.

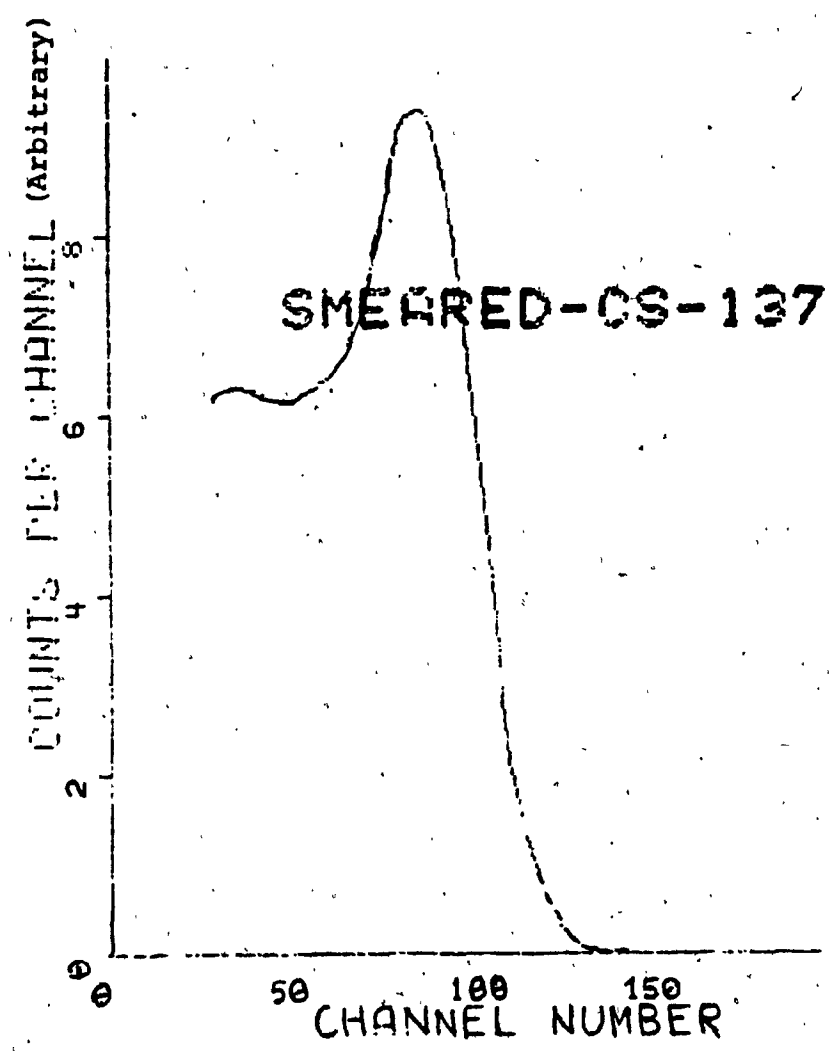


Figure 3.3 Smeared Monte Carlo spectrum for
 ^{137}Cs , one channel = 5 KeV

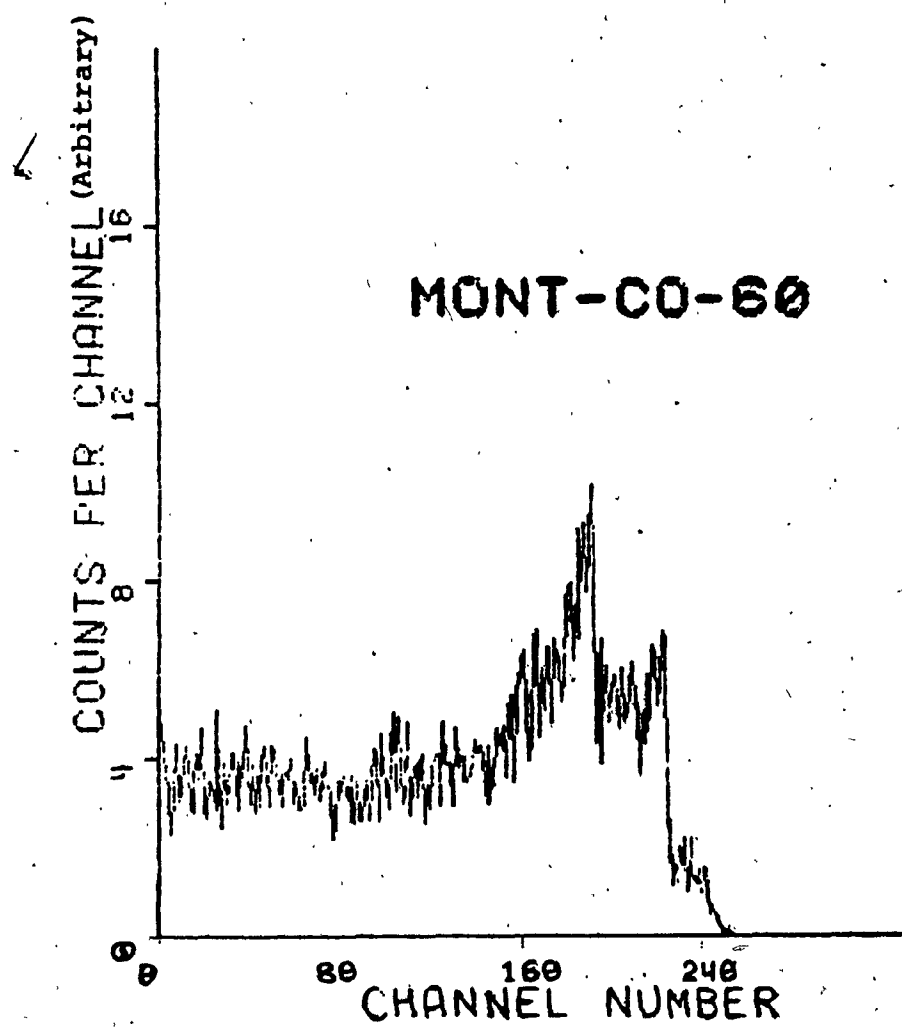


Figure 3.4 Monte Carlo spectrum for ^{60}Co ,
one channel=5 KeV.

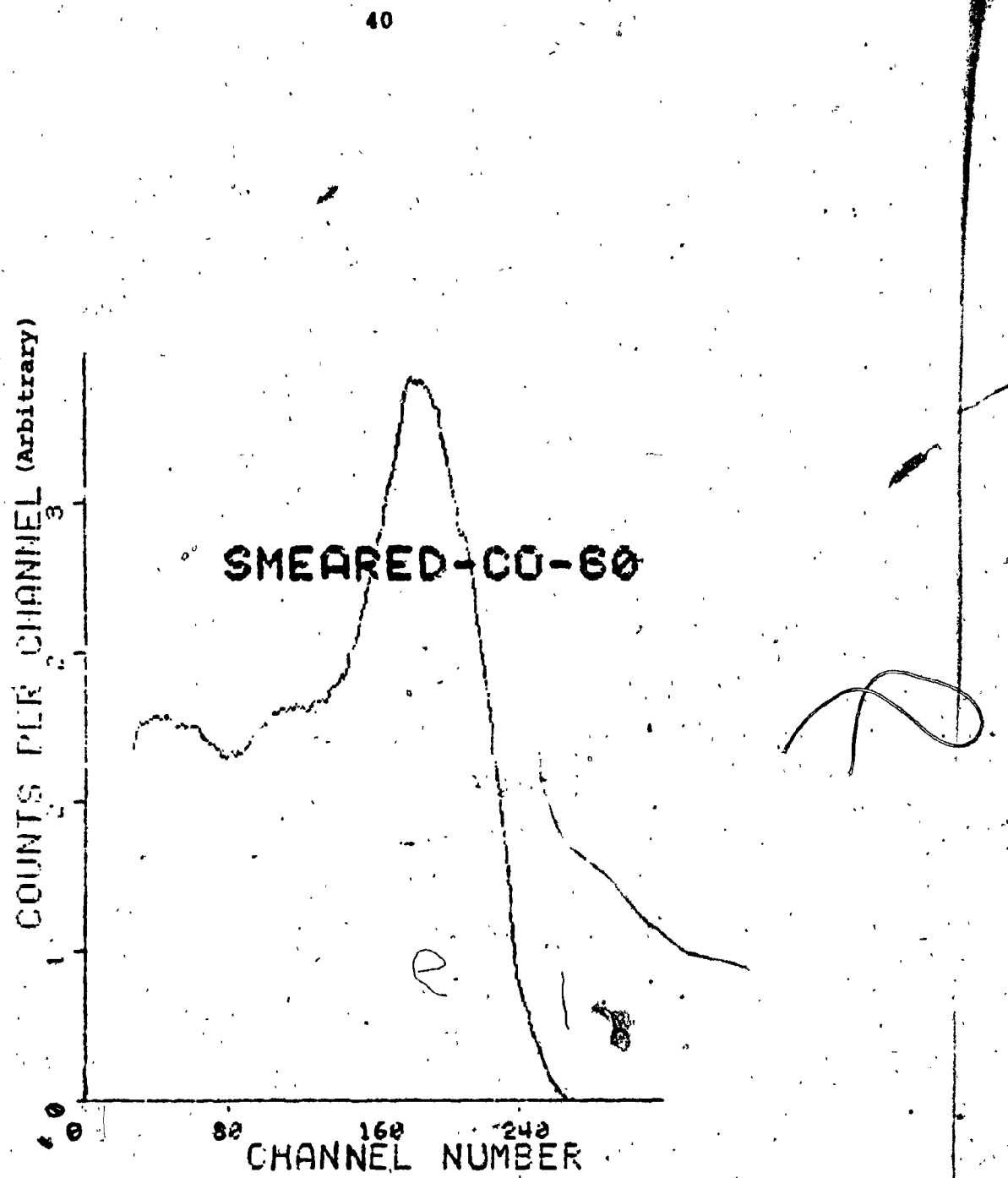


Figure 3.5 Smeared Monte Carlo spectrum for ^{60}Co ,
one channel=5 KeV.

Table 3.1

The cross sections of photoelectric(pe), Compton(Comp), pair production (pp) and total, in barns/atom.

Hydrogen

| Photon energy (MeV) | pe | Comp | pp | Total |
|---------------------|-----------|-----------|-----------|--------------|
| .10E-02 | .1140E+02 | .8520E-01 | .0000E+00 | .1148520E+02 |
| .15E-02 | .2930E+01 | .1650E+00 | .0000E+00 | .3095000E+01 |
| .20E-02 | .1110E+01 | .2480E+00 | .0000E+00 | .1358000E+01 |
| .30E-02 | .2810E+00 | .3780E+00 | .0000E+00 | .6590000E+00 |
| .40E-02 | .1060E+00 | .4670E+00 | .0000E+00 | .5730000E+00 |
| .50E-02 | .4940E-01 | .5170E+00 | .0000E+00 | .5664000E+00 |
| .60E-02 | .2630E-01 | .5490E+00 | .0000E+00 | .5750000E+00 |
| .80E-02 | .9790E-02 | .5830E+00 | .0000E+00 | .5927900E+00 |
| .10E-01 | .4550E-02 | .5990E+00 | .0000E+00 | .6035500E+00 |
| .15E-01 | .1160E-02 | .6090E+00 | .0000E+00 | .6101600E+00 |
| .20E-01 | .4160E-03 | .6070E+00 | .0000E+00 | .6074160E+00 |
| .30E-01 | .1020E-03 | .5920E+00 | .0000E+00 | .5921020E+00 |
| .40E-01 | .3760E-04 | .5760E+00 | .0000E+00 | .5760376E+00 |
| .50E-01 | .1730E-04 | .5590E+00 | .0000E+00 | .5590173E+00 |
| .60E-01 | .9160E-05 | .5440E+00 | .0000E+00 | .5440092E+00 |
| .80E-01 | .3370E-05 | .5160E+00 | .0000E+00 | .5160034E+00 |
| .10E+00 | .1550E-05 | .4920E+00 | .0000E+00 | .4920015E+00 |
| .15E+00 | .3770E-06 | .4430E+00 | .0000E+00 | .4430004E+00 |
| .20E+00 | .1380E-06 | .4060E+00 | .0000E+00 | .4060001E+00 |
| .30E+00 | .3360E-07 | .3530E+00 | .0000E+00 | .3530000E+00 |
| .40E+00 | .1230E-07 | .3170E+00 | .0000E+00 | .3170000E+00 |
| .50E+00 | .5650E-08 | .2890E+00 | .0000E+00 | .2890000E+00 |
| .60E+00 | .2990E-08 | .2670E+00 | .0000E+00 | .2670000E+00 |
| .80E+00 | .1100E-08 | .2350E+00 | .0000E+00 | .2350000E+00 |
| .10E+01 | .0000E+00 | .2110E+00 | .0000E+00 | .2110000E+00 |
| .15E+01 | .0000E+00 | .1720E+00 | .4400E-04 | .1720440E+00 |
| .20E+01 | .0000E+00 | .1460E+00 | .1170E-03 | .1461170E+00 |
| .30E+01 | .0000E+00 | .1150E+00 | .5110E-03 | .1155110E+00 |
| .40E+01 | .0000E+00 | .9620E-01 | .9940E-03 | .9719400E-01 |
| .50E+01 | .0000E+00 | .8310E-01 | .1430E-02 | .8453000E-01 |

Table 3.2

The cross sections of photoelectric(pe), Compton(Comp), pair production (pp) and total, in barns/atom.

Carbon

| Photon energy (MeV) | pe | Comp | pp | Total |
|---------------------|-----------|-----------|-----------|--------------|
| .10E-02 | .4350E+05 | .3000E+00 | .0000E+00 | .4350030E+05 |
| .15E-02 | .1380E+05 | .5900E+00 | .0000E+00 | .1380590E+05 |
| .20E-02 | .5980E+04 | .8990E+00 | .0000E+00 | .5980899E+04 |
| .30E-02 | .1780E+04 | .1430E+01 | .0000E+00 | .1781430E+04 |
| .40E-02 | .7400E+03 | .1820E+01 | .0000E+00 | .7401820E+03 |
| .50E-02 | .3710E+03 | .2090E+01 | .0000E+00 | .3730900E+03 |
| .60E-02 | .2080E+03 | .2290E+01 | .0000E+00 | .2102900E+03 |
| .80E-02 | .7990E+02 | .2550E+01 | .0000E+00 | .8245000E+02 |
| .10E-01 | .3930E+02 | .2740E+01 | .0000E+00 | .4204000E+02 |
| .15E-01 | .1060E+02 | .3030E+01 | .0000E+00 | .1363000E+02 |
| .20E-01 | .4140E+01 | .3190E+01 | .0000E+00 | .7330000E+01 |
| .30E-01 | .1100E+01 | .3300E+01 | .0000E+00 | .4400000E+01 |
| .40E-01 | .4230E+00 | .3300E+01 | .0000E+00 | .3723000E+01 |
| .50E-01 | .2010E+00 | .3250E+01 | .0000E+00 | .3451000E+01 |
| .60E-01 | .1110E+00 | .3190E+01 | .0000E+00 | .3301000E+01 |
| .80E-01 | .4240E-01 | .3050E+01 | .0000E+00 | .3092400E+01 |
| .10E+00 | .1990E-01 | .2920E+01 | .0000E+00 | .2939900E+01 |
| .15E+00 | .5160E-02 | .2650E+01 | .0000E+00 | .2655160E+01 |
| .20E+00 | .2070E-02 | .2430E+01 | .0000E+00 | .2432070E+01 |
| .30E+00 | .5700E-03 | .2120E+01 | .0000E+00 | .2120570E+01 |
| .40E+00 | .2230E-03 | .1900E+01 | .0000E+00 | .1900233E+01 |
| .50E+00 | .1080E-03 | .1730E+01 | .0000E+00 | .1730108E+01 |
| .60E+00 | .5980E-04 | .1600E+01 | .0000E+00 | .1600059E+01 |
| .80E+00 | .2370E-04 | .1410E+01 | .0000E+00 | .1410023E+01 |
| .10E+01 | .1160E-04 | .1270E+01 | .0000E+00 | .1270011E+01 |
| .15E+01 | .0000E+00 | .1030E+01 | .1600E-02 | .1031600E+01 |
| .20E+01 | .0000E+00 | .8780E+00 | .6440E-02 | .8844400E+00 |
| .30E+01 | .0000E+00 | .6900E+00 | .1860E-01 | .7086000E+00 |
| .40E+01 | .0000E+00 | .5770E+00 | .3080E-01 | .6078000E+00 |
| .50E+01 | .0000E+00 | .4980E+00 | .4190E-01 | .5399000E+00 |

Table 3.3

The cross sections of photoelectric(pe), Compton(Comp), pair production (pp) and total in cm^2/g .

NE102A Plastic

| Photon energy (MeV) | pe | Comp | pp | Total |
|---------------------|-------------|-------------|-------------|-------------|
| .10E-02 | .206259E+04 | .186793E-01 | .000000E+00 | .206261E+04 |
| .15E-02 | .654303E+03 | .366020E-01 | .000000E+00 | .654591E+03 |
| .20E-02 | .283523E+03 | .555928E-01 | .000000E+00 | .283579E+03 |
| .30E-02 | .843905E+02 | .875666E-01 | .000000E+00 | .844781E+02 |
| .40E-02 | .350781E+02 | .110711E+00 | .000000E+00 | .350892E+02 |
| .50E-02 | .175888E+02 | .126126E+00 | .000000E+00 | .177149E+02 |
| .60E-02 | .986102E+01 | .137282E+00 | .000000E+00 | .999829E+01 |
| .80E-02 | .378795E+01 | .151385E+00 | .000000E+00 | .393933E+01 |
| .10E-01 | .186314E+01 | .161229E+00 | .000000E+00 | .202437E+01 |
| .15E-01 | .502523E+00 | .175499E+00 | .000000E+00 | .678022E+00 |
| .20E-01 | .196266E+00 | .182979E+00 | .000000E+00 | .379245E+00 |
| .30E-01 | .521475E-01 | .187407E+00 | .000000E+00 | .239555E+00 |
| .40E-01 | .200530E-01 | .186570E+00 | .000000E+00 | .206623E+00 |
| .50E-01 | .952871E-02 | .183310E+00 | .000000E+00 | .192839E+00 |
| .60E-01 | .526214E-02 | .179682E+00 | .000000E+00 | .184944E+00 |
| .80E-01 | .201003E-02 | .171580E+00 | .000000E+00 | .173590E+00 |
| .10E+00 | .943384E-03 | .164162E+00 | .000000E+00 | .165105E+00 |
| .15E+00 | .244614E-03 | .148798E+00 | .000000E+00 | .149043E+00 |
| .20E+00 | .981296E-04 | .136434E+00 | .000000E+00 | .136532E+00 |
| .30E+00 | .270210E-04 | .118966E+00 | .000000E+00 | .118993E+00 |
| .40E+00 | .105713E-04 | .106653E+00 | .000000E+00 | .106664E+00 |
| .50E+00 | .511973E-05 | .971297E-01 | .000000E+00 | .971348E-01 |
| .60E+00 | .283481E-05 | .898161E-01 | .000000E+00 | .898189E-01 |
| .80E+00 | .112349E-05 | .791350E-01 | .000000E+00 | .791361E-01 |
| .10E+01 | .549865E-06 | .712428E-01 | .000000E+00 | .712433E-01 |
| .15E+01 | .000000E+00 | .578253E-01 | .781460E-04 | .579035E-01 |
| .20E+01 | .000000E+00 | .492596E-01 | .311393E-03 | .495710E-01 |
| .30E+01 | .000000E+00 | .387257E-01 | .908421E-03 | .396341E-01 |
| .40E+01 | .000000E+00 | .323854E-01 | .151200E-02 | .338974E-01 |
| .50E+01 | .000000E+00 | .279550E-01 | .206098E-02 | .300160E-01 |

Table 3.4

The cross sections of photoelectric(pe), Compton(Comp), pair production (pp) and total, in cm^2/g .

Muscle

| Photon energy (MeV) | pe | Comp | pp | Total |
|---------------------|-----------|-----------|-----------|--------------|
| .10E-02 | .4880E+01 | .2120E+00 | .0000E+00 | .5090000E+01 |
| .15E-01 | .1320E+01 | .2080E+00 | .0000E+00 | .1530000E+01 |
| .20E-01 | .5260E+00 | .2050E+00 | .0000E+00 | .7310000E+00 |
| .30E-01 | .1440E+00 | .1980E+00 | .0000E+00 | .3420000E+00 |
| .40E-01 | .5730E-01 | .1920E+00 | .0000E+00 | .2490000E+00 |
| .50E-01 | .2810E-01 | .1860E+00 | .0000E+00 | .2140000E+00 |
| .60E-01 | .1580E-01 | .1810E+00 | .0000E+00 | .1970000E+00 |
| .80E-01 | .6310E-02 | .1710E+00 | .0000E+00 | .1780000E+00 |
| .10E+00 | .3040E-02 | .1630E+00 | .0000E+00 | .1660000E+00 |
| .15E+00 | .8320E-03 | .1470E+00 | .0000E+00 | .1480000E+00 |
| .20E+00 | .3350E-03 | .1350E+00 | .0000E+00 | .1350000E+00 |
| .30E+00 | .9590E-04 | .1170E+00 | .0000E+00 | .1170000E+00 |
| .40E+00 | .4110E-04 | .1050E+00 | .0000E+00 | .1050000E+00 |
| .50E+00 | .2220E-04 | .9580E-01 | .0000E+00 | .9590000E-01 |
| .60E+00 | .1390E-04 | .8870E-01 | .0000E+00 | .8870000E-01 |
| .80E+00 | .6990E-05 | .7790E-01 | .0000E+00 | .7790000E-01 |
| .10E+01 | .4330E-05 | .7000E-01 | .0000E+00 | .7000000E-01 |
| .15E+01 | .2030E-05 | .5690E-01 | .9690E-04 | .5700000E-01 |
| .20E+01 | .1290E-05 | .4860E-01 | .3860E-03 | .4890000E-01 |
| .30E+01 | .7180E-06 | .3820E-01 | .1110E-02 | .3930000E-01 |
| .40E+01 | .4890E-06 | .3190E-01 | .1800E-02 | .3370000E-01 |
| .50E+01 | .3730E-06 | .2750E-01 | .2410E-02 | .3000000E-01 |

CHAPTER 4

CALCULATION OF DOSE.

This chapter outlines the relation between energy absorbed and exposure, gamma-flux and exposure, and calculation of the gamma ray constant. The response of plastic relative to muscle is described.

4.1 Exposure(X)¹¹.

The exposure X, is the quotient of dQ by dm, where dQ is the absolute value of the total charge of the ions of one sign produced in air when all electrons (negatrons and positrons) liberated by photons in a volume element of air whose mass is dm are completely absorbed,

$$X = dQ/dm$$

(4.1)

The special unit of exposure is Roentgen and $1R = 2.58 \times 10^{-4}$ Coulomb/kg of air.

4.2 Exposure rate.

The Exposure rate, \bar{X} , is the quotient of dX by dt where dX is the increment of exposure in time interval dt.

$$\bar{X} = dx/dt$$

A special unit of exposure rate is any quotient of the roentgen or its multiple or submultiple by a suitable unit of time (R/s, R/m, R/h, mR/h etc).

4.3 Absorbed dose.

Absorbed dose is defined as the quotient dE by dm where dE is the mean energy imparted by ionizing radiation to the mass dm of matter in the volume element,

$$D = dE / dm$$

(4.2)

The absorbed dose from gamma rays can be calculated if the transport and absorption of secondary electrons are included as well as the transport of the primary gamma rays, fluorescent X-rays, Compton scattered photons and annihilation quanta. However, the fluorescence X-rays and electrons are assumed to be stopped where they were generated.

The special unit of absorbed dose is Gray denoted by the symbol Gy,

$$1\text{Gy} = 1\text{J kg}^{-1} = 100 \text{ rad}$$

4.4 Absorbed dose rate.

The absorbed dose rate, \bar{D} , is the quotient of dD by dt where dD is the increment of absorbed dose in time interval dt .

$$\bar{D} = dD/dt$$

A special unit of absorbed dose rate is any quotient of the rad or its multiple or submultiple by a suitable unit of time (rad/s, rad/m, rad/h, mrad/h etc).

4.5 Calculation of absorbed dose from gamma radiation.

In principle, the calculation of absorbed dose is rather simple. One determines the photon flux density at the point of interest, multiply the energy of photons to get the energy flux density and then by the mass energy absorption coefficient to determine how much of the energy is actually deposited at the point of interest. Finally, applying the appropriate constant to convert the units into rads or Gy and multiplying by the time during which the photon flux density was present yields absorbed dose. Mathematically,

$$D(\text{rad}) = 1.6 \times 10^{-8} \phi(\text{cm}^{-2} \text{ sec}^{-1}) E(\text{MeV}) \mu_{\text{en}}/\rho(\text{cm}^{-2}/\text{g}) t(\text{sec})$$

In actual practice, however, the calculation of absorbed dose is very difficult and complex. To use the

above equation, we have to make some approximations, such as all photons have same energy and photon interactions are absorptive. The basic cause of the difficulties is the fact that not all photon interactions are purely absorptive.

We have to account for the energy spectrum of the photons since in general the source will not be monoenergetic. Even if it were, there will be an energy distribution of that photon passing through the medium.

In flux density calculation, we have to consider absorption and scattering, so we use the Monte Carlo method which yields^a more accurate calculation of dose.

4.6 Relation between gamma flux density and exposure rate.

One Roentgen is equivalent to $2.58 \cdot 10^{-4}$ Coul/(kg of air)

$$\begin{aligned}
 1R &= 2.58 \cdot 10^{-7} \text{ Coul}/(\text{gm of air}) \\
 &= 2.58 \cdot 10^{-7} / 1.602 \cdot 10^{-19} \text{ ion pairs/gm air} \\
 &= (1.6121 \cdot 10^{12} / \text{gm}) (34 \text{ eV/ion pair}) \\
 &= (5.482 \cdot 10^{13} \text{ eV/gm}) (1.602 \cdot 10^{-12} \text{ erg/eV}) \\
 &= 87.7 \text{ erg/gm} \\
 &= 87.7 \cdot 10^{-2} \text{ rad} \\
 &= 87.7 \cdot 10^{-4} \text{ Gy}
 \end{aligned}$$

(4.3)

The absorbed energy in air at a point where the exposure is 1R is 87.7 ergs/gm. The absorbed dose at a point in air where exposure is R Roentgen is given by

$$D_{\text{air}} = 87.7 \cdot 10^{-4} \text{ Gy}$$

(4.4)

The number of rad per Roentgen in air is 0.877. When the medium involved is other than air, and if electronic equilibrium exists, then dose in the medium is

$$D_m = 0.877 (\mu_{en}/\rho)_{\text{med}} / (\mu_{en}/\rho)_{\text{air}} \text{ rad}$$

(4.5)

Total energy per square cm corresponding to a dose rate of one Roentgen is given as

$$E_f = 87.7 / (\mu_{en}/\rho)_{\text{air}} \text{ ergs/cm}^2 \cdot \text{R}$$

(4.6)

where E_f = energy fluence incident per Roentgen($\text{ergs/cm}^2 \cdot \text{R}$)
and (μ_{en}/ρ) = mass energy absorption coefficient(cm^2/gm).

The absorbed energy in units of ergs per gms is given as

$$E_f (\mu_{en}/\rho)_{\text{air}} = 1.602 \cdot 10^{-6} \Phi E (\mu_{en}/\rho)_{\text{air}}$$

(4.7)

where Φ = particle fluence and E is the energy of photon.

The number of photons per square cm per Roentgen, a quantity obtained by dividing equation (4.6) by energy of photon,

$$\begin{aligned}
 E_f/E &= 87.7/E(\mu_{en}/\rho)_{air} \text{ ergs/MeV cm}^2\text{-R} \\
 &= 87.7/[1.602 \cdot 10^{-6.9} E(\mu_{en}/\rho)_{air}] \text{ photons/cm}^2\text{-R} \\
 &= 5.475 \cdot 10^7 / E(\mu_{en}/\rho)_{air} \text{ photons/cm}^2\text{-R}
 \end{aligned}
 \tag{4.8}$$

The number of photons/sec-cm² corresponding to a dose rate of one Roentgen/hr can be calculated from the following equation

$$R/\text{hr} = 5.475 \cdot 10^7 / E(\mu_{en}/\rho)_{air} (3.6 \cdot 10^3) \text{ photons/sec-cm}^2
 \tag{4.9}$$

4.7 Specific gamma ray constant, Γ .

The exposure rate for gamma-radiation has usually been taken as equivalent to $I(\mu_{en}/\rho)$, where I is the gamma ray intensity and (μ_{en}/ρ) is the mass energy absorption coefficient of air for the particular energy involved. The constant Γ is determined by calculating the absorbed dose rate for the flux density of photons produced at a distance of one meter through an area of one cm² from a source, which has activity 1 mCi. The photon absorption along the air

path from source to the point in question is assumed negligible. The specific gamma ray constant Γ at one meter can be calculated from the following formula¹⁵

$$\begin{aligned} \Gamma = & 3.7 \cdot 10^7 (\text{disintegration/sec-mCi}) \cdot 3.6 \cdot 10^3 (\text{sec/h}) \\ & 10^6 (\text{eV/Mev}) \cdot 4.803 \cdot 10^{-10} (\text{esu/electron}) \cdot 1.293 \cdot 10^{-3} (\text{g/cm}^3 \text{ air}) \\ & (1/(4\pi \cdot 10^4 \text{ cm}^2)) (1/34) (\text{ion pair per eV}) \cdot (h\nu_i (\text{MeV}/\gamma\text{-ray})) \\ n_i (\gamma\text{-rays/disintegration}) \cdot (\nu_{en}/\rho)_i \text{ cm}^2/\text{g} \\ = & 19.36 \sum n_i (h\nu)_i (\nu_{en}/\rho)_i \text{ mR/mCi-hr at one meter.} \end{aligned}$$

(4.10)

where n_i photons of energy $(h\nu)_i$ are emitted per disintegration, and the average energy W to form an ion pair in air has been assumed to be 34.0 eV. Later the values of Γ will be calculated for various isotopes to check the accuracy of the Monte Carlo method.

4.8 The energy absorbed in the plastic scintillator is independent of incident photon energy.

To calculate a proportionality factor (K), between the total energy absorbed by the scintillator and the total energy incident, the Monte Carlo program was run for 10,000 photons of energies between 50 keV to 1250 keV. The number of incident photons at the incident energy corresponding to

10,000 interacted photons is calculated from the relation,

$$N = N_0(1 - \exp(-\mu d))$$

$$N_0 = N / (1 - \exp(-\mu d))$$

(4.11)

where N_0 = Number of incident photons

N = Number of interacted photons

μ = total attenuation coefficient

and d = detector thickness.

If we denote $N(E)$ the number of counts at the energy E of the Monte Carlo energy spectrum, and N_0 the number of incident photons of energy E each, incident on the detector, then the proportionality constant K , may be defined as

$$K(E) = \Sigma N(E)E / N_0 E_0$$

(4.12)

The values of K calculated are shown in the table 4.1. The maximum difference of K 's from each other is less than 10%. The K values are plotted as a function of incident energy, shown in figure 4.1. Thus the absorbed energy in NE102A plastic scintillator is independent of incident radiation energy.

Table 4.1

The proportionality constant (K) between the total energy absorbed and total energy incident on NE102A plastic scintillator.

| Energy of incident photon (MeV) | N(E)E (MeV) | K |
|--|----------------|------|
| .50E-01 | .1149E+03 | .143 |
| .10E+00 | .2214E+03 | .126 |
| .20E+00 | .5549E+03 | .139 |
| .30E+00 | .9969E+03 | .151 |
| .40E+00 | .1479E+04 | .155 |
| .50E+00 | .1996E+04 | .155 |
| .60E+00 | .2556E+04 | .156 |
| .70E+00 | .3106E+04 | .155 |
| .80E+00 | .3708E+04 | .153 |
| .90E+00 | .4276E+04 | .151 |
| .10E+01 | .4890E+04 | .148 |
| .125E+01 | .1113E+05 | .161 |

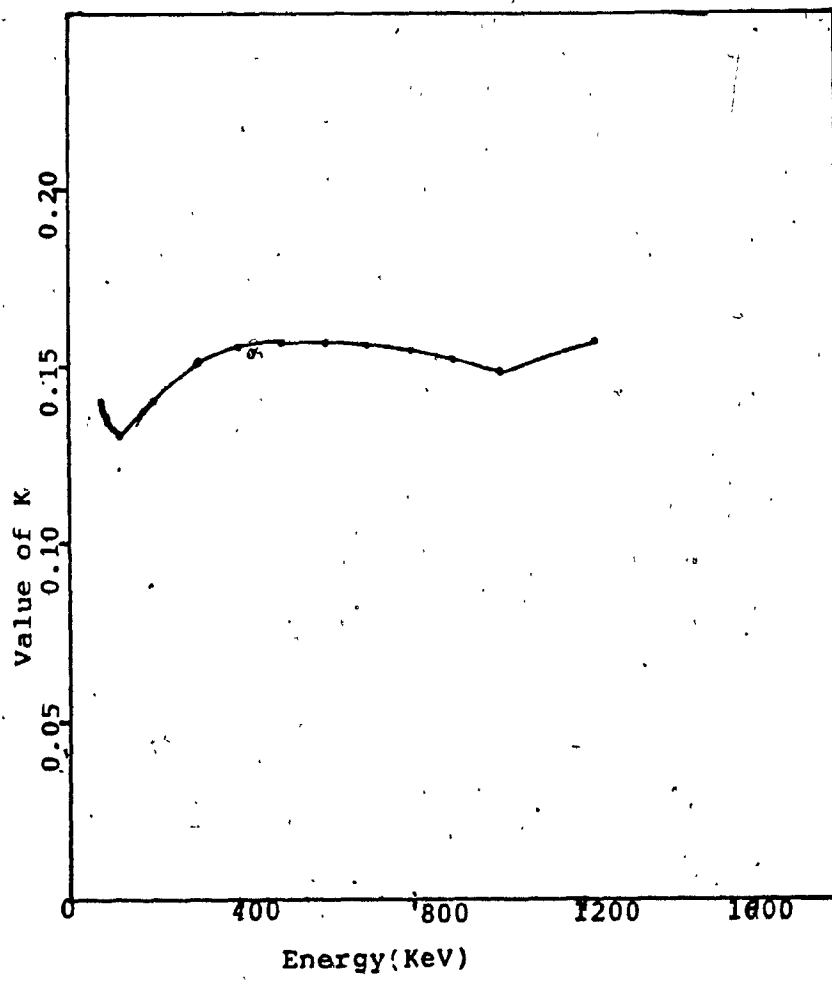


Figure 4.1 The ratio(K) between the total energy absorbed and total energy incident is independent of incident photon energy.

The relatively constant value of K as a function of energy can be explained as

$$K(E) = \sum N(E) E / N_0 E_0$$

$$= \bar{N}E / N_0 E_0$$

$$= \bar{E}N_0(1 - \exp(-\mu d)) / N_0 E_0$$

$$= (\bar{E}/E_0)(1 - \exp(-\mu d))$$

(4.13)

where (\bar{E}/E_0) is increasing slowly with E_0 where as $(1 - \exp(-\mu d))$ is slowly decreasing and the product that is K, is varying slowly with the incident photon energy.

4.9 Response of plastic scintillator relative to muscle.

Mass-energy absorption coefficient is a measure of incident photons undergoing absorption, thus it determines the energy absorbed by the medium and, therefore dose. Ionization in a free-air chamber is the standard process for measuring gamma-ray response. The response of a free-air chamber as a function of photon energy is nearly proportional to the product of energy fluence and mass energy absorption coefficient (μ_{en}/ρ)_{air} in cm²/gm. The usual way of expressing the energy-dependence of a scintillation detector for photons is to compare its response with that of a free air chamber. The ratios of mass energy absorption coefficients of two media as a function of energies will yield a response curve with respect to one another. The

response will not be correct because scattering of photons in the media involved were not taken into account in the mass energy absorption coefficient. The response can be calculated by taking the ratios of energy absorbed in the media as a function of incident photon energy. An investigation has been made to calculate the response of plastic scintillator with respect to muscle due to photons from 50 KeV to 1330 KeV in order to compare with the calculated ratios of mass energy absorption coefficients of plastic and muscle.

The mass energy absorption coefficient (μ_{en}/ρ) for C, H, O, N and air were taken from Hubbel¹⁶, and given in table 4.2. The mass energy absorption coefficient for plastic was determined according to the ratio H:C=1.104¹⁷ and that for tissue according to the weight percent elemental composition defined by ICRU¹⁸ as 10.2% H, 12.3% C, 3.5% N, and 72.9% O. The mass energy absorption coefficients of NE102A plastic scintillator and muscle are given in table 4.3. The plot of the ratios of $(\mu_{en}/\rho)_{\text{plastic}} / (\mu_{en}/\rho)_{\text{muscle}}$ shown in figure 4.2a as a function of energy. Since the response from mass energy absorption coefficients is not correct as explained, the Monte Carlo method is used to determine the energy absorbed in the plastic and in the muscle. The ratios of energy absorbed per incident photon in plastic and muscle, as a function of incident energies will give true response.

Table 4.2

Mass energy-absorption coefficients, μ_{m}/ρ in cm^2/g .

| Photon energy (MeV) | H | C | N | O | Air |
|---------------------------|-----------|-----------|-----------|-----------|-----------|
| .10E-02 | .6823E+01 | .2216E+04 | .3312E+04 | .4588E+04 | .3608E+04 |
| .15E-02 | .1753E+01 | .6738E+03 | .1089E+04 | .1560E+04 | .1199E+04 |
| .20E-02 | .6652E+00 | .2907E+03 | .4781E+03 | .6942E+03 | .5287E+03 |
| .30E-02 | .1697E+00 | .8641E+02 | .1442E+03 | .2140E+03 | .1607E+03 |
| .40E-02 | .6564E-01 | .3589E+02 | .6032E+02 | .9105E+02 | .7602E+02 |
| .50E-02 | .3288E-01 | .1798E+02 | .3041E+02 | .4645E+02 | .3901E+02 |
| .60E-02 | .2002E-01 | .1016E+02 | .1726E+02 | .2659E+02 | .2245E+02 |
| .80E-02 | .1161E-01 | .4089E+01 | .6955E+01 | .1095E+02 | .9261E+01 |
| .10E-01 | .9854E-01 | .2003E+01 | .3445E+01 | .5447E+01 | .4648E+01 |
| .15E-01 | .1102E-01 | .5425E+00 | .9421E+00 | .1507E+01 | .1304E+01 |
| .20E-01 | .1355E-01 | .2159E+00 | .3751E+00 | .6023E+00 | .5266E+00 |
| .30E-01 | .1864E-01 | .6407E-01 | .1069E+00 | .1687E+00 | .1504E+00 |
| .40E-01 | .2315E-01 | .3264E-01 | .4932E-01 | .7365E-01 | .6705E-01 |
| .50E-01 | .2709E-01 | .2360E-01 | .3160E-01 | .4335E-01 | .4038E-01 |
| .60E-01 | .3053E-01 | .2078E-01 | .2517E-01 | .3164E-01 | .3008E-01 |
| .80E-01 | .3620E-01 | .2029E-01 | .2199E-01 | .2451E-01 | .2394E-01 |
| .10E+00 | .4063E-01 | .2143E-01 | .2225E-01 | .2347E-01 | .2319E-01 |
| .15E+00 | .4812E-01 | .2448E-01 | .2470E-01 | .2504E-01 | .2494E-01 |
| .20E+00 | .5255E-01 | .2655E-01 | .2664E-01 | .2678E-01 | .2672E-01 |
| .30E+00 | .5695E-01 | .2869E-01 | .2872E-01 | .2877E-01 | .2872E-01 |
| .40E+00 | .5859E-01 | .2949E-01 | .2951E-01 | .2953E-01 | .2949E-01 |
| .50E+00 | .5899E-01 | .2968E-01 | .2969E-01 | .2971E-01 | .2966E-01 |
| .60E+00 | .5875E-01 | .2955E-01 | .2956E-01 | .2957E-01 | .2952E-01 |
| .80E+00 | .5739E-01 | .2885E-01 | .2885E-01 | .2886E-01 | .2882E-01 |
| .10E+01 | .5555E-01 | .2791E-01 | .2791E-01 | .2508E-01 | .2787E-01 |
| .15E+01 | .5074E-01 | .2548E-01 | .2548E-01 | .2458E-01 | .2545E-01 |
| .20E+01 | .4649E-01 | .2343E-01 | .2345E-01 | .2346E-01 | .2342E-01 |
| .30E+01 | .3992E-01 | .2046E-01 | .2054E-01 | .2063E-01 | .2055E-01 |
| .40E+01 | .3523E-01 | .1848E-01 | .1848E-01 | .1880E-01 | .1868E-01 |
| .50E+01 | .3175E-01 | .1709E-01 | .1733E-01 | .1756E-01 | .1739E-01 |

Table 4.3

*Mass energy-absorption coefficients, μ_{en}/ρ in cm^2/g .

| Photon energy (MeV) | Plastic NE102A | Muscle | Air | Plastic Air ratio | Muscle Air ratio |
|---------------------------|-------------------|-----------|-----------|----------------------|---------------------|
| .10E-02 | .2032E+04 | .3738E+04 | .3608E+04 | .5632E+00 | .1036E+01 |
| .15E-02 | .6178E+03 | .1260E+04 | .1199E+04 | .5153E+00 | .1051E+01 |
| .20E-02 | .2666E+03 | .5593E+03 | .5287E+03 | .5042E+00 | .1058E+01 |
| .30E-02 | .7923E+02 | .1719E+03 | .1607E+03 | .4930E+00 | .1070E+01 |
| .40E-02 | .3291E+02 | .7300E+02 | .7602E+02 | .4329E+00 | .9603E+00 |
| .50E-02 | .1649E+02 | .3719E+02 | .3901E+02 | .4226E+00 | .9533E+00 |
| .60E-02 | .9316E+01 | .2127E+02 | .2245E+02 | .4150E+00 | .9473E+00 |
| .80E-02 | .3749E+01 | .8741E+01 | .9261E+01 | .4049E+00 | .9439E+00 |
| .10E-01 | .1845E+01 | .4353E+01 | .4648E+01 | .3969E+00 | .9366E+00 |
| .15E-01 | .4983E+00 | .1201E+01 | .1304E+01 | .3821E+00 | .9210E+00 |
| .20E-01 | .1991E+00 | .4807E+00 | .5266E+00 | .3780E+00 | .9129E+00 |
| .30E-01 | .6032E-01 | .1367E+00 | .1504E+00 | .4011E+00 | .9087E+00 |
| .40E-01 | .3189E-01 | .6187E-01 | .6706E-01 | .4755E+00 | .9226E+00 |
| .50E-01 | .2394E-01 | .3842E-01 | .4038E-01 | .5928E+00 | .9514E+00 |
| .60E-01 | .2164E-01 | .2965E-01 | .3008E-01 | .7195E+00 | .9856E+00 |
| .80E-01 | .2167E-01 | .2485E-01 | .2394E-01 | .9054E+00 | .1038E+01 |
| .10E+00 | .2310E-01 | .2469E-01 | .2319E-01 | .9960E+00 | .1065E+01 |
| .15E+00 | .2653E-01 | .2706E-01 | .2494E-01 | .1064E+01 | .1085E+01 |
| .20E+00 | .2880E-01 | .2911E-01 | .2672E-01 | .1078E+01 | .1089E+01 |
| .30E+00 | .3114E-01 | .3135E-01 | .2872E-01 | .1084E+01 | .1091E+01 |
| .40E+00 | .3201E-01 | .3219E-01 | .2949E-01 | .1085E+01 | .1092E+01 |
| .50E+00 | .3222E-01 | .3240E-01 | .2966E-01 | .1086E+01 | .1092E+01 |
| .60E+00 | .3208E-01 | .3225E-01 | .2952E-01 | .1087E+01 | .1092E+01 |
| .80E+00 | .3132E-01 | .3148E-01 | .2882E-01 | .1087E+01 | .1092E+01 |
| .10E+01 | .3030E-01 | .3045E-01 | .2787E-01 | .1087E+01 | .1093E+01 |
| .15E+01 | .2767E-01 | .2714E-01 | .2545E-01 | .1087E+01 | .1067E+01 |
| .20E+01 | .2543E-01 | .2557E-01 | .2342E-01 | .1086E+01 | .1092E+01 |
| .30E+01 | .2215E-01 | .2237E-01 | .2055E-01 | .1078E+01 | .1088E+01 |
| .40E+01 | .1993E-01 | .2024E-01 | .1868E-01 | .1067E+01 | .1083E+01 |
| .50E+01 | .1836E-01 | .1877E-01 | .1739E-01 | .1056E+01 | .1079E+01 |

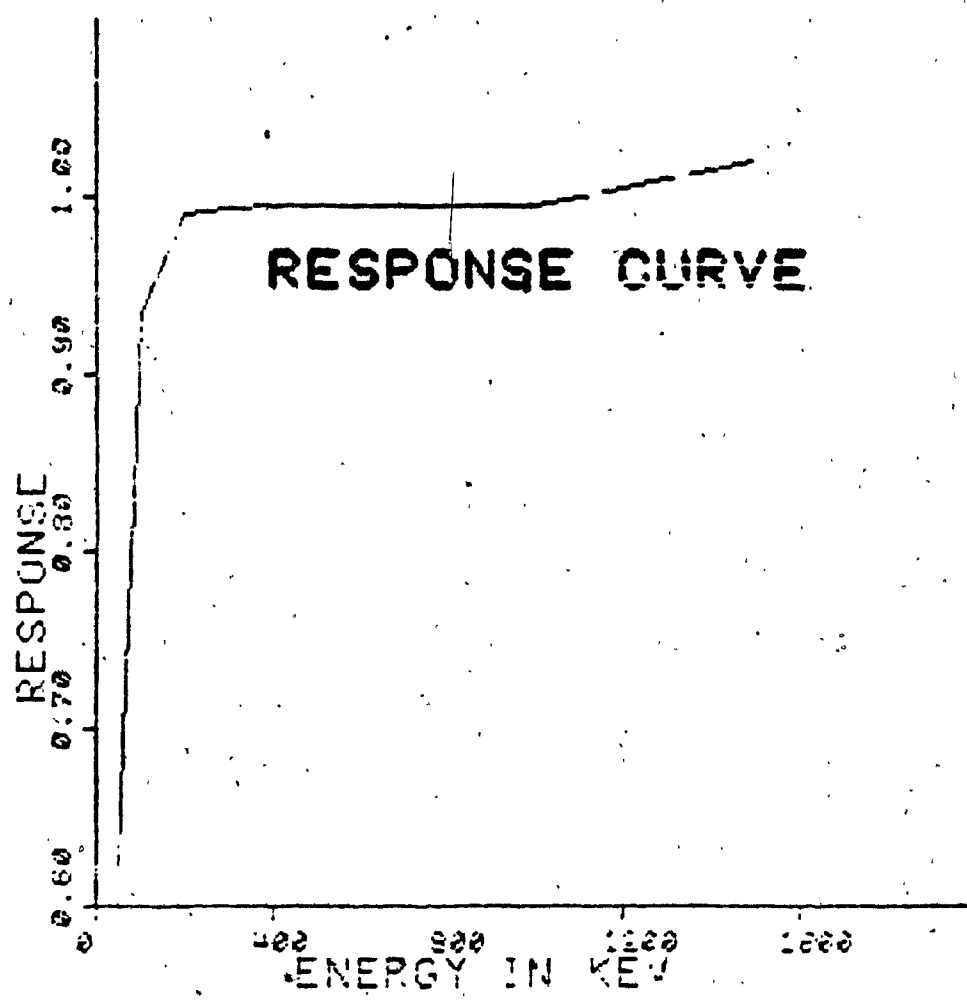


Figure 4.2a Plot of $(\nu_{en}/\rho)_{\text{plastic}} / (\nu_{en}/\rho)_{\text{muscle}}$ as a function of photon energy.

The Monte Carlo program was run for photon energies between 50 keV to 1330 KeV with a 5.08 cm detector thickness for 10,000 photons. The number of photons to be interacted in muscle (NIPM) was determined compared with plastic by using the relation (4.14), so that the number of incident photons in both plastic and muscle would be the same

$$NIPM = \{(1 - \exp(-\mu_m d)) / (1 - \exp(-\mu_p d))\} 10000$$

(4.14)

where μ_m and μ_p are the interpolated total attenuation coefficients for muscle and plastic respectively, corresponding to the incident photon energy. The Monte Carlo program was run for those number of photons (NIPM) in muscle. To calculate dose response a program DOSE was developed. The dose per incident photon per unit mass was determined by taking the sum of the product of the number of photons in the energy channel with the corresponding energy of the channel in the initially determined Monte Carlo spectrum, and then dividing by the mass of detector and total number of incident photons. This dose calculation was done by the subroutines PSDOS and TSDOS for plastic and muscle respectively and the ratio of dose was determined, shown in table 4.4. The plot of the ratios of doses in plastic and in muscle as a function of incident photon energies is shown in figure 4.2b.

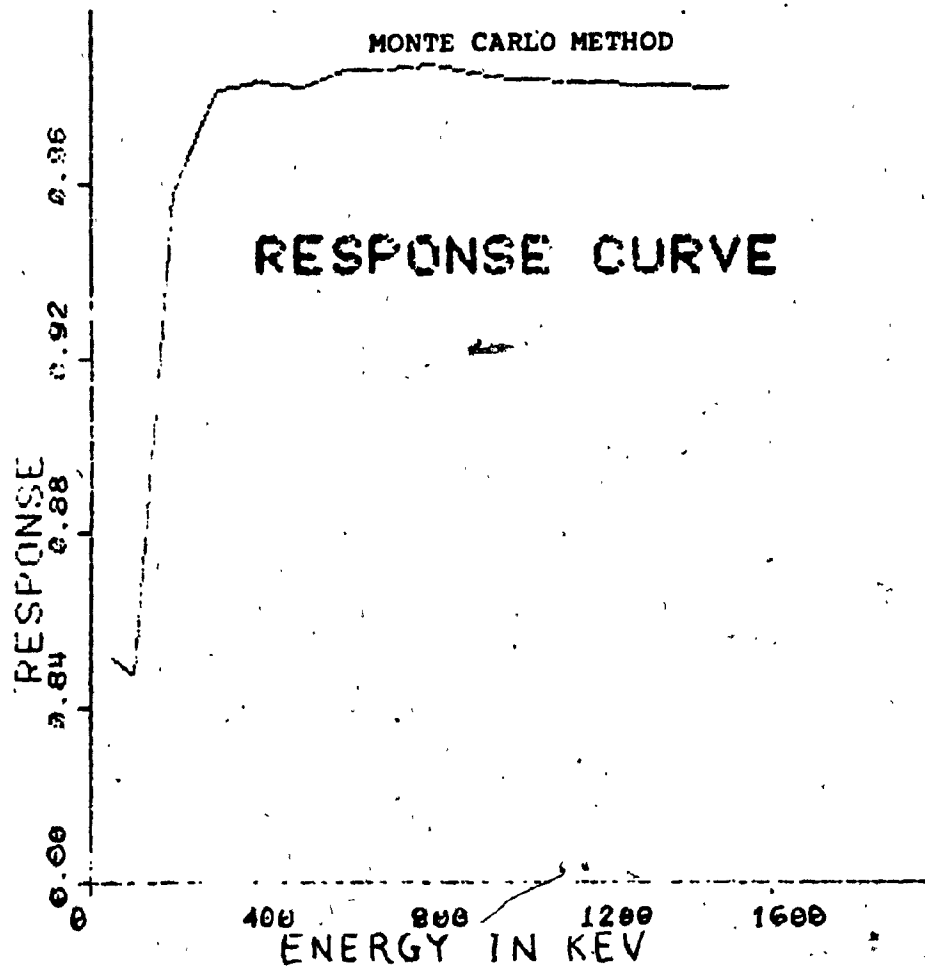


Figure 4.2b Plot of the ratio of energy absorbed in plastic and muscle by Monte Carlo method, as a function of energy.

Table 4.4**The response (R) of NE102A plastic relative to muscle.**

| Energy of incident photon. (MeV) | R |
|---|------|
| .50E-01 | .851 |
| .10E+00 | .847 |
| .20E+00 | .958 |
| .30E+00 | .981 |
| .40E+00 | .983 |
| .50E+00 | .982 |
| .60E+00 | .986 |
| .70E+00 | .986 |
| .80E+00 | .987 |
| .90E+00 | .985 |
| .10E+01 | .984 |

4.10 Accuracy of Monte Carlo program.

To check the Monte Carlo program whether it yields correct results, a comparison has been made between the dose in Roentgen/photon, calculated from Monte Carlo and the dose in Roentgen/photon, calculated from the equation (4.10) for a specific gamma ray constant for the energies 50 KeV to 1330 KeV. The doses are within 10% except for 50 KeV where it is more than 23%, shown in table 4.5. From the results, it implies that the Monte Carlo program is correct.

Table 4.5

The gamma dose in Roentgen/photon calculated from gamma-ray constant (Γ) and from Monte Carlo method for NE102A plastic scintillator.

| Energy of photon | γ -dose/photon from γ -ray constant | γ -dose/photon from Monte Carlo |
|------------------------|---|--|
| (MeV) | (R/photon) | (R/photon) |
| .50E-01 | .2941E-15 | .3835E-15 |
| .10E+00 | .3378E-15 | .3246E-15 |
| .20E+00 | .7783E-15 | .7140E-15 |
| .30E+00 | .1255E-14 | .1157E-14 |
| .40E+00 | .1718E-14 | .1580E-14 |
| .50E+00 | .2160E-14 | .1985E-14 |
| .60E+00 | .2580E-14 | .2389E-14 |
| .70E+00 | .2978E-14 | .2766E-14 |
| .80E+00 | .3358E-14 | .3131E-14 |
| .90E+00 | .3715E-14 | .3463E-14 |
| .125E+1 | .4854E-14 | .4613E-14 |

CHAPTER 5

EXPERIMENTAL TECHNIQUE

The block diagram of experimental set up used in this investigation is shown in figure 5.1.

The description of detector assembly, amplification system, data accumulation, linearity of detection system, spectrum transfer and the method of calibration of the plastic detector are given in this chapter.

5.1 Detector assembly.

The detector used is a cylindrical 2"x 2" NE102A plastic scintillator, manufactured by Nuclear Enterprises Ltd. According to the manufacturer it has an excellent balance of properties, high light output (65% anthracine), good light transmission (2.5 m technical attenuation length), fast decay time (2.4 nanosecond), ratio H:C atoms is 1.104 and the density is 1.032 gm/cm^3 . The photomultiplier used is the 9626/8D8/DM1-2, also supplied by Nuclear Enterprises. For detector bias, we used a high voltage regulated power supply model 2K-10.

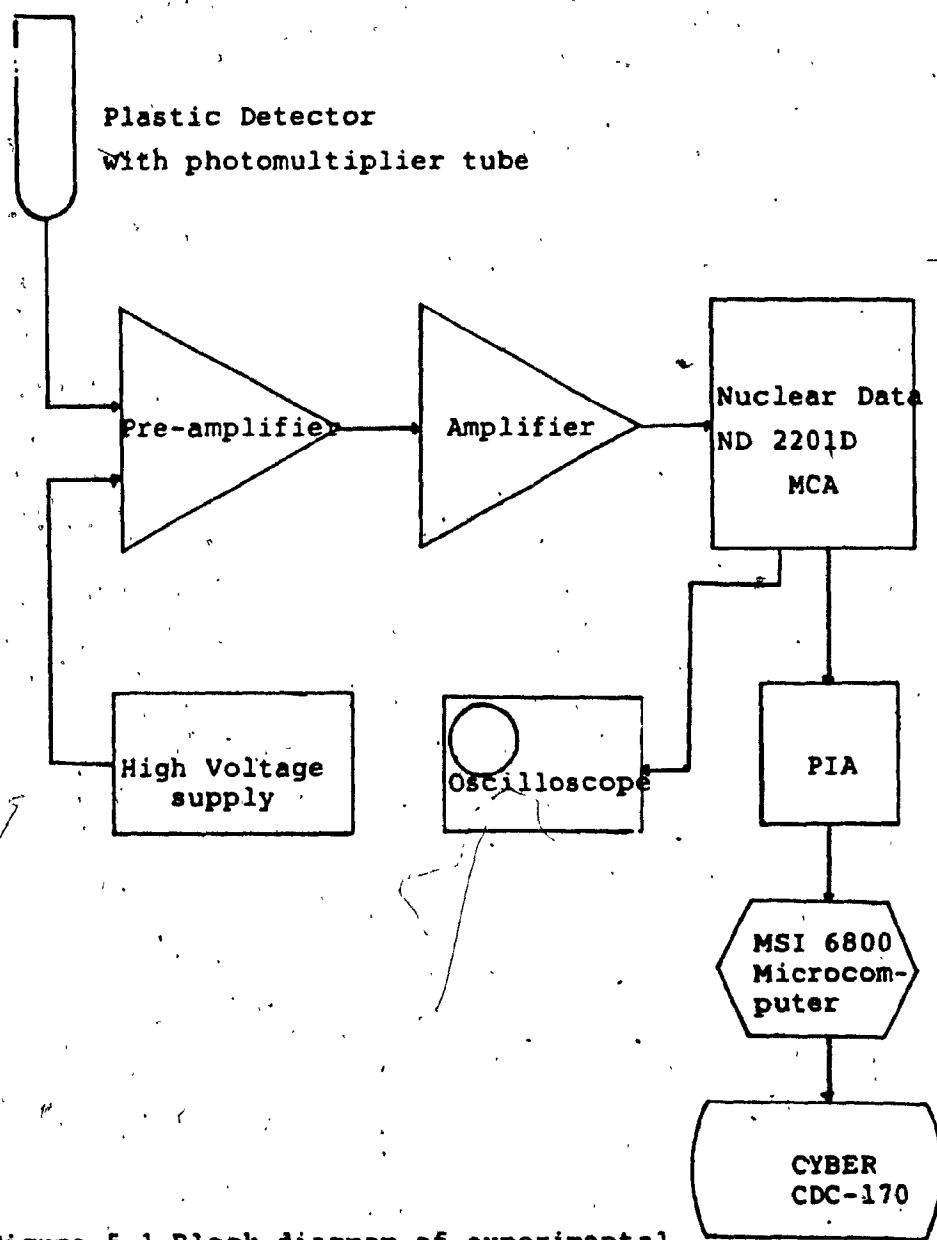


Figure 5.1 Block diagram of experimental setup.

Power Design Pacific, Inc.

5.2 Amplification system.

The system consists of a preamplifier model 401 FET of Mech-Tronics, Nuclear Corporation and a linear amplifier model M-31 of Simtec Ltd. The preamplifier circuit requires 8 mAmp from -24 Volts supplied through a 1 kohm load resistor which was provided externally. The conversion gain of the preamplifier is 100 mV/picocoulomb. The course gain was set at 64 and fine gain at 1 on the amplifier. The preamplifier pulses are amplified and shaped in the linear amplifier.

5.3 Data accumulation.

The data for our experiment was collected with a Nuclear Data ND-2201D series MCA with 100 megahertz 8192 channel analog-to-digital converter (ADC). The conversion gain was set at 1024. The lower cut-off for the spectrum has been chosen on the analog-to-digital converter (ADC) so that the influence of electronic noise is negligible. The lower level discriminator was set at about 9 mV.

5.4 Linearity of detection system.

The linearity of the system with amplifier and 1000 channels pulse height analyzer was tested with a BNC ramp pulse generator model LG-1 and pulser model BH-1. The curve is shown in figure 5.2. The upper channel of ^{60}Co spectrum is about 278.

If the analyzer is linear, an equal number of counts will be stored in each channel and the plot will be a straight line. Deviation from the straight line is an indication of differential nonlinearity. The differential nonlinearity (DNL) of an analyzer may be computed by:

$$\text{DNL} = 100(1 - N_x / N_{av})$$

where N_x = number of counts in channel x . N_{av} = average number of counts in all channels.

The differential non-linearity over channels 1 to 400 is 5 %.

5.5 Spectrum transfer.

A MSI6800 (SS-50 bus) microcomputer was used to transfer the spectrum from the MCA-memory to the Cyber 170 (main University computer) via leased telephone line for analysis. The MSI6800 is linked with MCA by a Parallel

SYS-LINEARITY

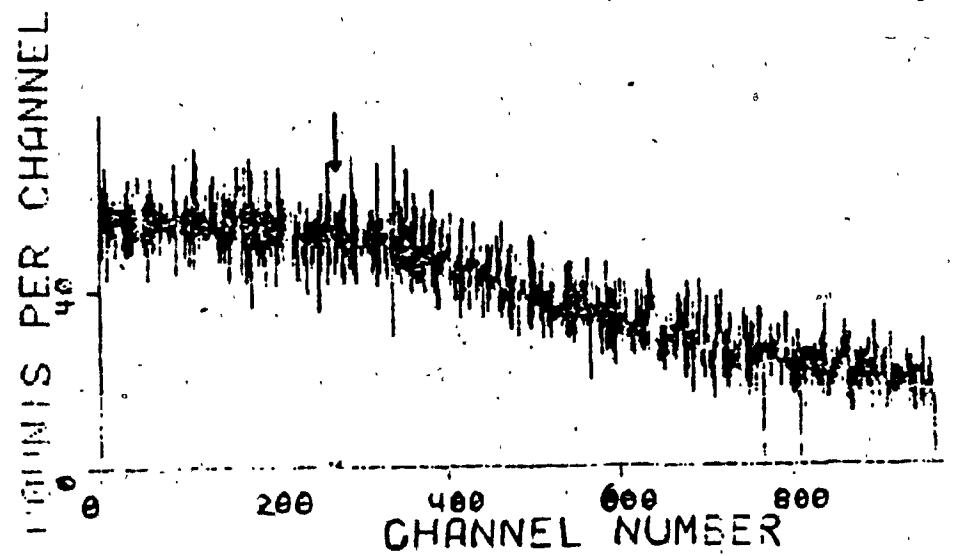


Figure 5.2 Linearity of detection system, upper
channel of ^{60}Co is about 278 as shown.

Interface Adapter(PIA) board connected via long ribbon cable to the "printer" B connector of the MCA. A program MCAINTER (written by Nicole Ranger and modified by Dr. N. Eddy) is used to read the spectrum into the memory of the MSI6800 from the memory of the MCA.

5.6 Calibration of detector.

In detector materials with high atomic numbers (Z) and reasonable size, the total energy absorption peak (photopeak) is observed. However, with low Z materials in the energy range up to 5 MeV, the primary interaction is essentially Compton scattering. There was therefore no total energy absorption peak found in the gamma ray spectrum of the NE102A plastic scintillator. Due to multiple scattering and statistical broadening of the response spectrum, the "Compton edge" is not represented by a sharp edge in the spectrum. The calibration of energy response of the system was done by a method based on obtaining an agreement between the results of Monte Carlo calculations of energy response and the experimental spectra for ^{137}Cs and ^{60}Co . The energy corresponding to a channel in experimental spectrum is known from Monte Carlo spectrum and subsequently an energy calibration curve (KeV/channel) was constructed.

Experimental spectra were collected for the sources ^{137}Cs (0.6616 MeV) and ^{60}Co (1.17 and 1.33 MeV), shown in figures 5.3 and 5.5 respectively. The response spectra initially determined by Monte Carlo calculations for ^{137}Cs and ^{60}Co were smeared out by using Gaussian resolution function as described in section 3.7. The calculated and experimental spectra were then normalized for the same number of photons. Both spectra were plotted by adjusting x-values by trial and error until best agreement was obtained. Here the x-value is the energy in the Monte Carlo spectrum and channel number in the experimental spectrum. Figures 5.4 and 5.6 are for the sources ^{137}Cs and ^{60}Co respectively. Using the half-height and mid-point of the Compton peak, the calibration curves were constructed, shown in figures 5.7 and 5.8 respectively. From both curves, the energy per channel was found to be identical, and equal to 6.1 KeV/channel.

5.7 Dose determination with plastic scintillator.

The spectrum has to be collected for a specified time with the plastic scintillator. The energy per channel is known from the calibration curve. The number of counts in each channel is to be multiplied by the energy of each channel and the response, which will give the total energy deposited in the detector for that specified time. The

total energy of the spectrum divided by the mass of the detector and the time of collection of the spectrum, which is then multiplied by a conversion factor to convert it into dose in units of rad per unit time or Gy per unit time or Roentgen per unit time.

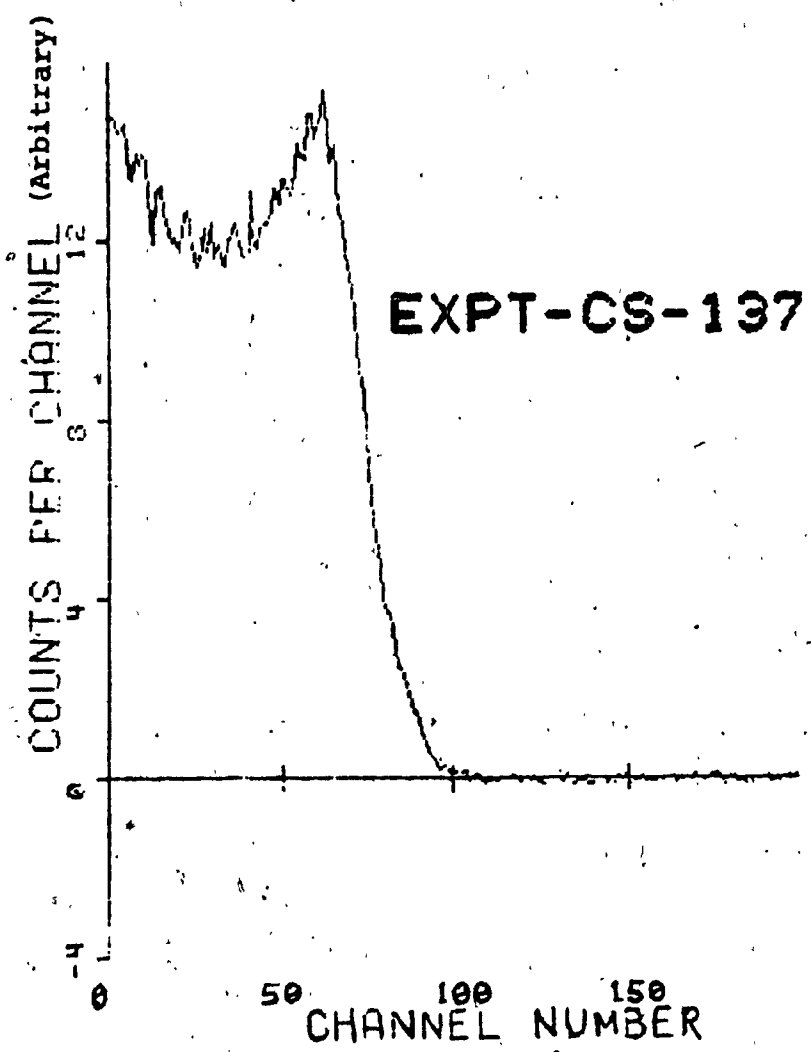


Figure 5.3 Experimental spectrum of ^{137}Cs .
(background subtracted)

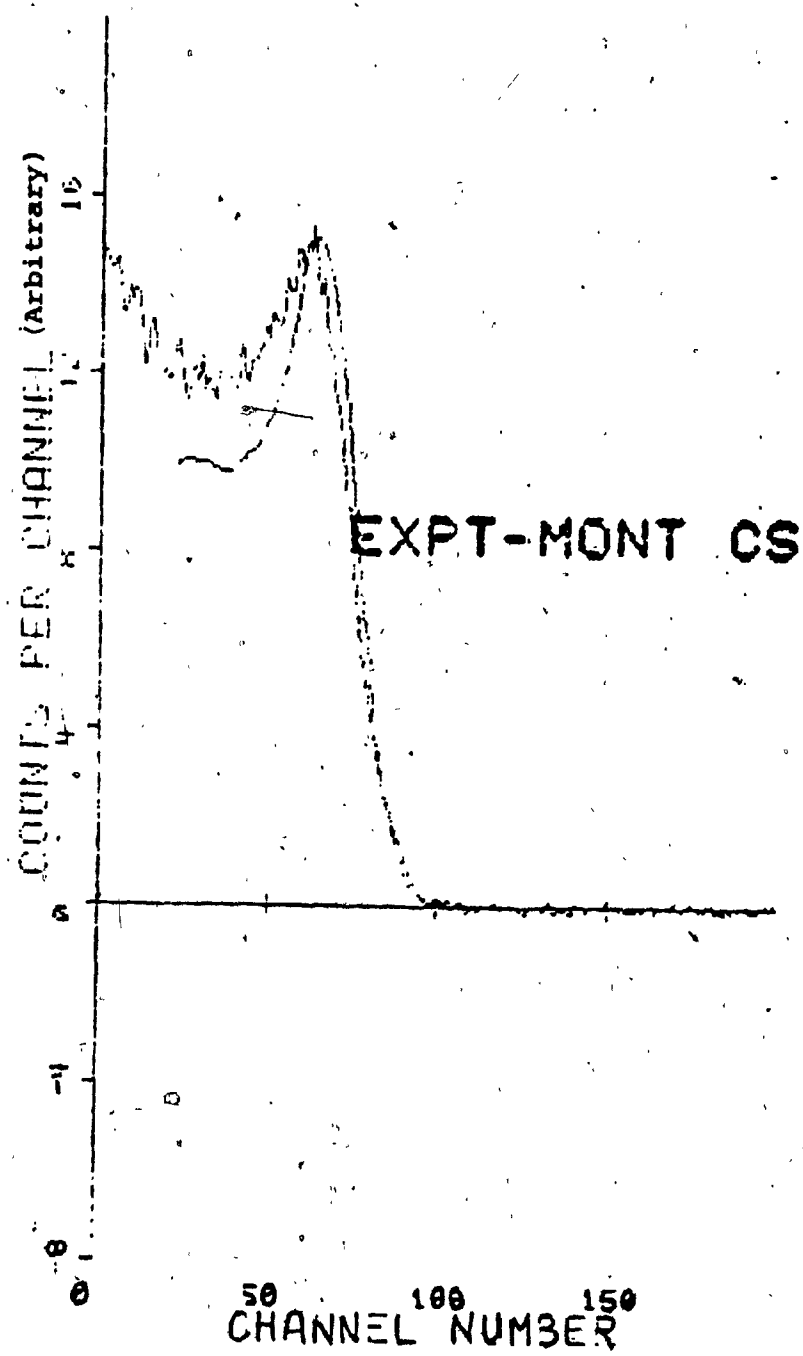


Figure 5.4 Experimental and smeared Monte Carlo spectra for ^{137}Cs . 1 experimental channel = 0.73 Monte Carlo channel.

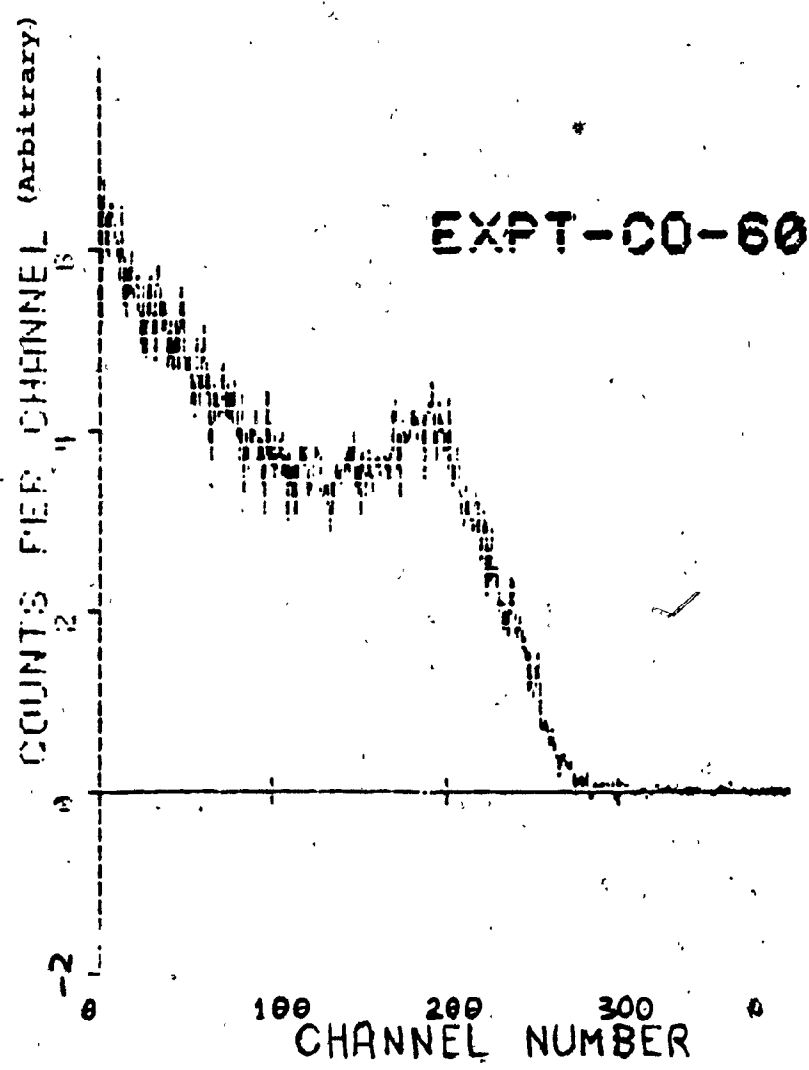


Figure 5.5 Experimental spectrum for ^{60}Co .
(background subtracted).

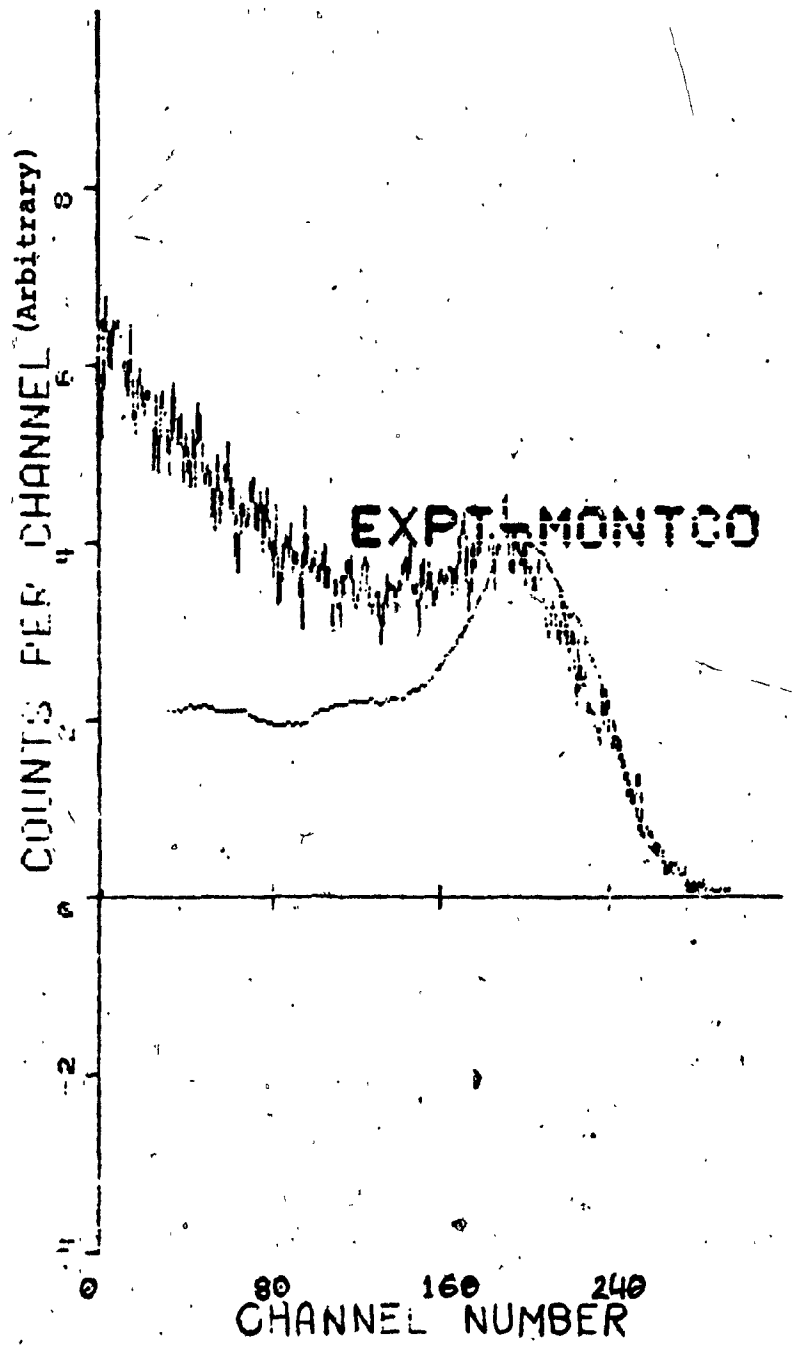


Figure 5.6 Experimental and smeared Monte Carlo spectra for ^{60}Co . 1 experimental channel = 1.07 Monte Carlo channel.

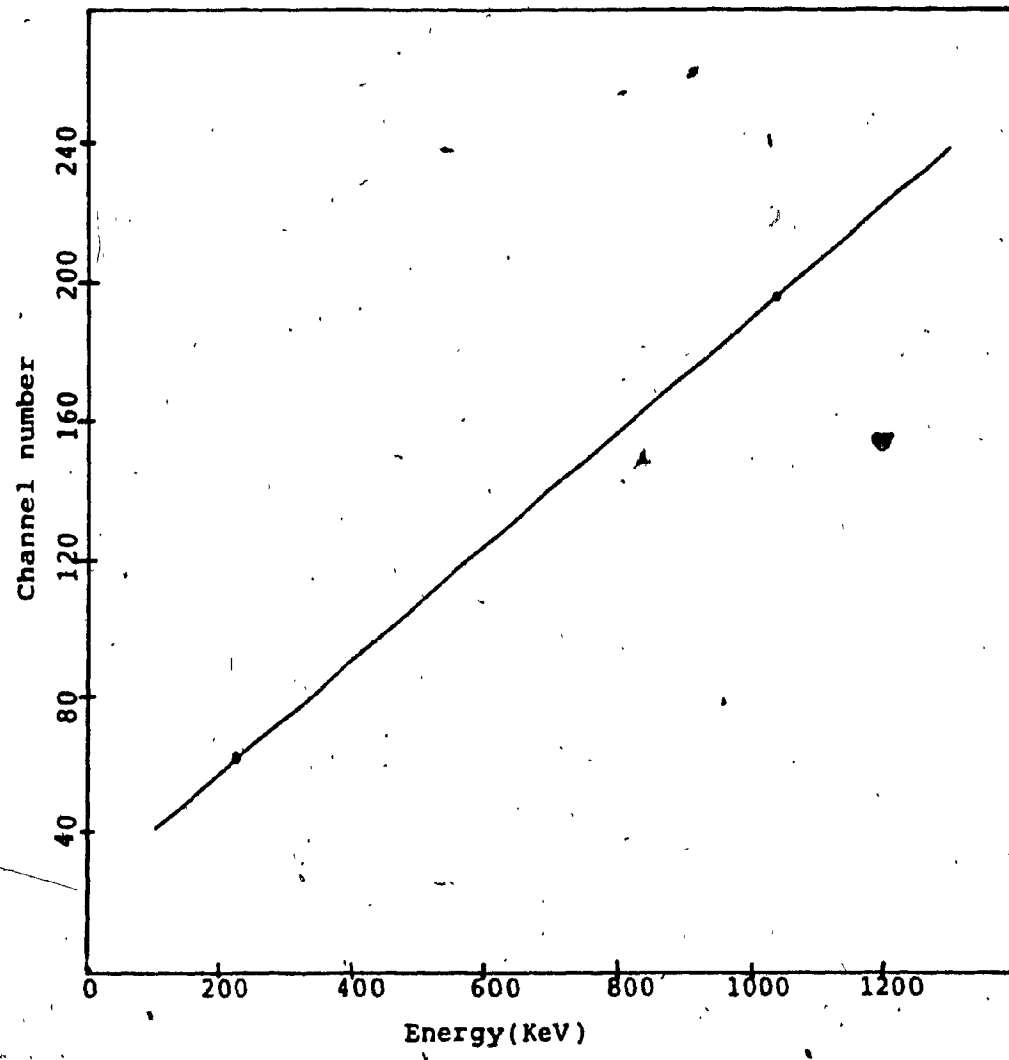


Figure 5.7 The calibration curve of plastic detector
(using mid-point of spectra).

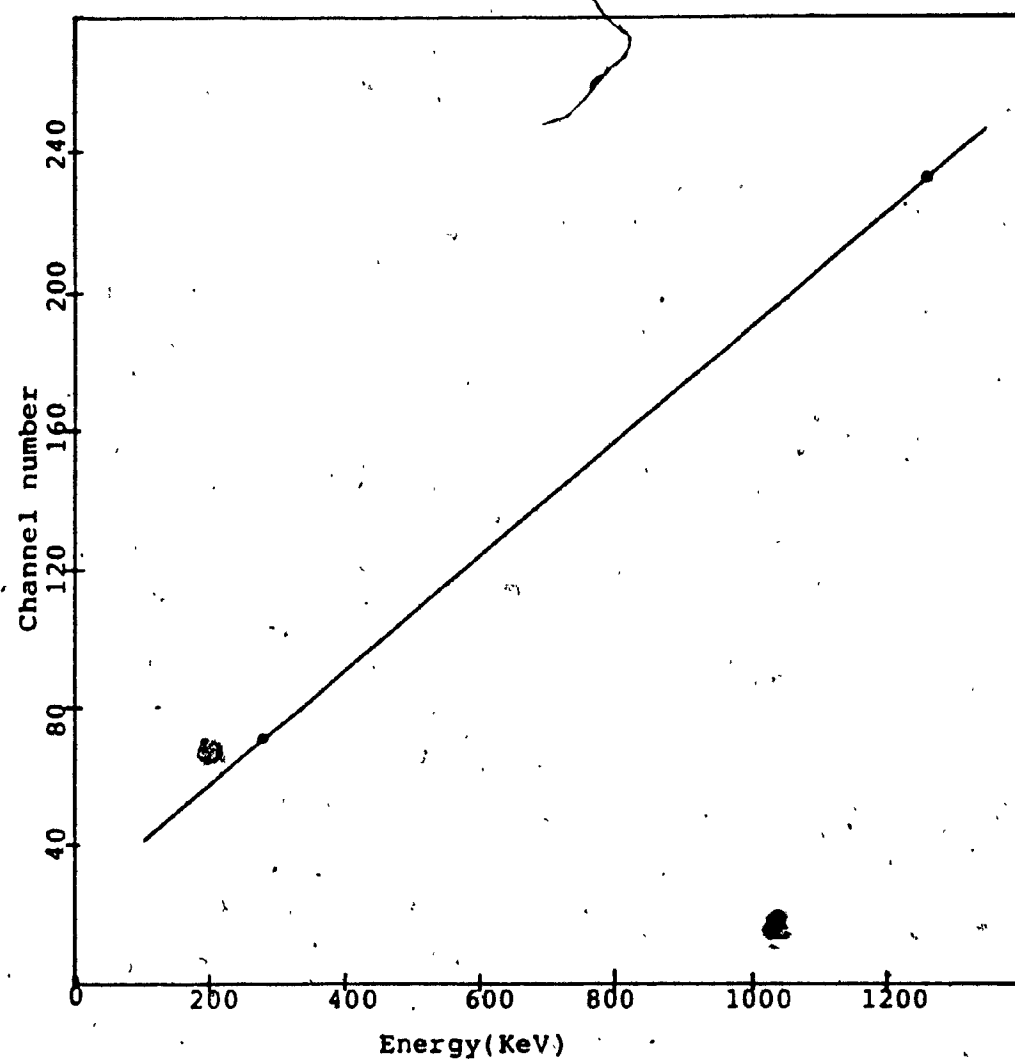


Figure 5.8 The calibration curve of plastic detector
(using half-height of spectra).

CHAPTER 6

BACKGROUND RADIATION

The importance of knowing the radiation of natural origin lies in the fact that mankind has always been exposed to natural background radiation at chronic low level doses. The doses due to natural origin can be used as standard reference to those due to artificial sources.

The doses to human beings due to externally incident radiation vary with the type of soil and the area, and therefore with the type of rock from which it was derived. The terrestrial gamma ray dose inside the buildings will, in general, be different from the value outdoors, owing to the different radioactive content of the building materials and attenuation effects of the walls for the radiation from outside the building. Studies of these effects have been made by Spiers et al¹⁹.

The measurements of background radiation spectra were made at Concordia University, Montreal with the NE102A plastic scintillator. A typical background spectrum collected for 1,000 secs is shown in figure 6.1. These spectra were used in the program BKGRND to calculate the radiation dose in rad/h or Roentgen/h. The number

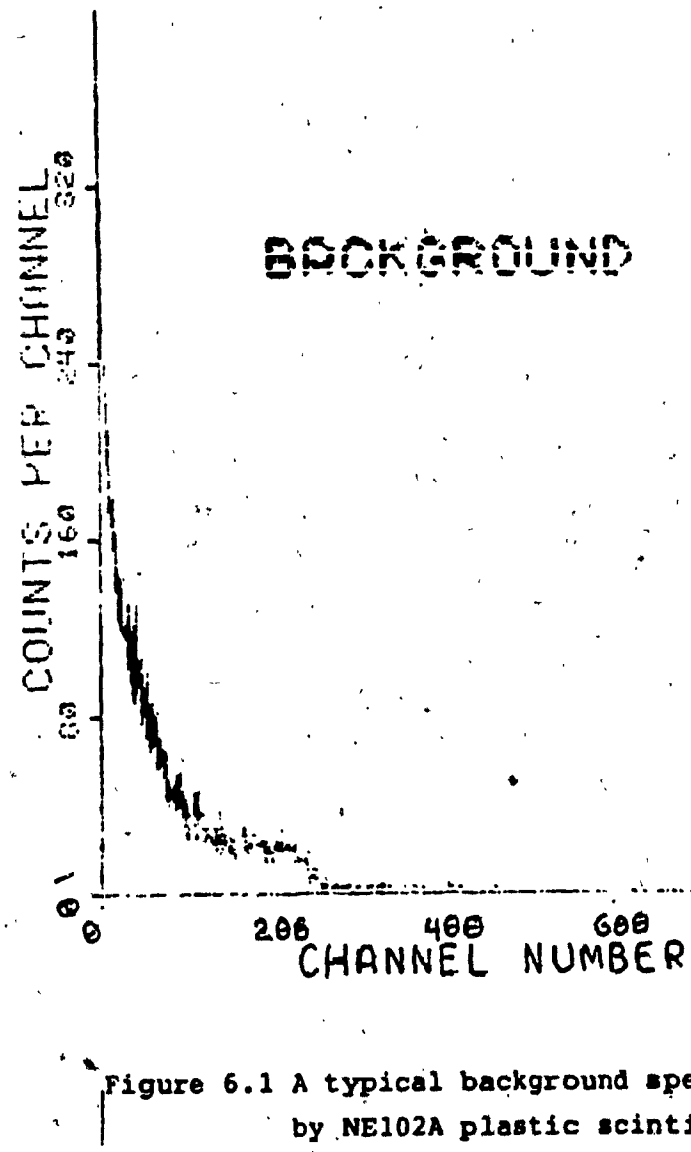


Figure 6.1 A typical background spectrum measured by NE102A plastic scintillator.

of counts in each channel is multiplied by the corresponding energy of each channel and then by the response which gave the energy spectrum. The energy per channel is obtained from the calibration curve. The energy of the spectrum is summed and converted into micro-rad/h or micro-roentgen/h. The daily variation of background radiation in micro-roentgen/h is shown in the figure 6.2. All samples were collected between 12.00 and 2.00 P.M.

The measured background here at Montreal is compared with world wide averages of radiation level estimated by Hanson and Komarov²⁰ based on the data from the UNSCEAR report²¹. Their estimated values for indoor dose rate range between 2 and 9 micro-rad/h. The measured background radiation with plastic scintillator ranged from 1.8 micro-rad/h (2 micro-Roentgen/h) to 9.6 micro-rad/h (10 micro-Roentgen/h).

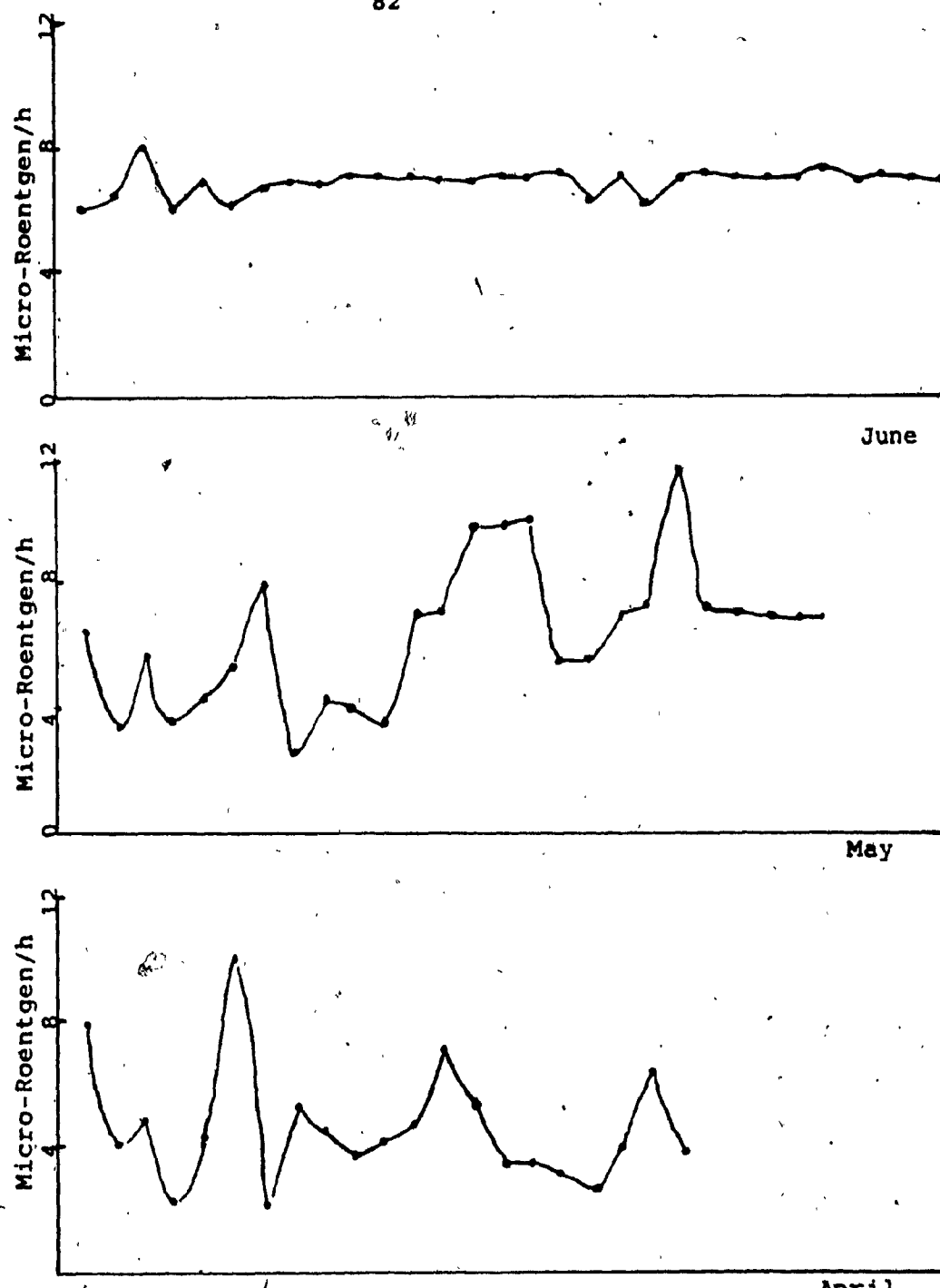


Figure 6.2 Daily variation of background radiation.

CHAPTER 7

DISCUSSIONS

The results obtained from the Monte Carlo calculations and the experiment indicate good agreement between them, as shown in figures 5.4 and 5.6. The energy absorbed in the scintillator is independent of incident photon energy so it can be used to measure dose where the energy spectrum is unknown and the response is also good in the energy range of our interest. The energy independent measurement of absorbed dose of gamma rays of any survey meter is always desirable.

Background spectra were measured for 400 sec, 1000 sec, 4000 sec, 8000 sec, 40000 sec, and 80000 sec to test how much time it would take to measure background radiation. All results are within 2% of each measurement, so 400 sec (5 to 6 minutes) can be used to measure background.

The background radiation measured with the NE102A plastic detector is in good agreement with published values.

The ionization chamber²² is among the oldest devices used in radiation measurement. In order to provide the necessary independence of radiation energy, ionization chambers are the method of choice for the measurement of

total dose. The early investigations of natural radiation were made using ionization chambers with electrometers as the recording instruments but this technique was superseded, on the grounds of speed and convenience of measurement, by an instrument of a type originally designed by Sievert which uses an electrometer tube circuit to provide a direct reading. Sievert's instrument consists of an 8-liter steel ionization chamber containing nitrogen at 30 atm, and has a sensitivity sufficient to enable a measurement of background dose rate to be made in a period of less than 1 minute²³. Owing to the difference in atomic composition between wall and filling gas and because of ion recombination effects, considerable care is necessary in the derivation of absolute measurements in terms of absorbed dose in tissue with this type instrument. For tissue-equivalent ionization chambers, a mixture of gases is required. Since it is usually impractical to provide mixed gases in continuous flow, these chambers are ordinarily filled and sealed off. The gas is then slowly absorbed or adsorbed by the chamber components, which means that gas pressure and the sensitivity of the chamber will decrease with time. Another complication may arise if one of the gases is preferentially absorbed faster than the others.



Geiger counters have been widely used for the detection of gamma radiation at natural levels. However, their response varies markedly with photon energies and they

can not be used with an accuracy as dose-rate meters except where the energy spectrum is well known.

Advantages of plastic scintillator.

Plastic scintillators usually have very short recovery time (of the order of tens of nsecs) enabling the plastic scintillator to be used in conjunction with a fast photomultiplier tube to provide scintillation detectors with time resolutions of less than 10^{-9} sec. Plastic scintillator permits great flexibility in size and shape of radiation detector elements, such as thin foil, fine filaments, tubes, beads and massive blocks. This property enables high gamma ray detection efficiency to be obtained using large scintillation volumes. Such detectors can provide cheap, large volume devices for integral-spectrum counting or very simple γ -ray spectrometry. They have been used for assaying bulky clinical samples with high efficiency as well as for body radioactivity measurements^{24,25}.

The large hydrogen content of plastic scintillators allows them to be used for fast neutron detection and spectrometry by absorption of scintillations due to recoil protons within the materials. The solid detector is effectively 1000 times bigger than the gas detector of the same physical size so the count rates are correspondingly higher.

Disadvantages of plastic detector.

The main disadvantages associated with scintillation detectors are electrical. High voltage power supplies must be stable to prevent gain changes in the photomultiplier tube. They also require more precise preamplifier, amplifier and pulse height analysis circuits. Due to the high count rate associated with high efficient and fast pulses, pulse pile up and sorting can be a problem. This can be alleviated by using a fast PHA system.

Extreme humidity and temperature are often bothersome while variations in temperature alter the electronic noise produced at the photocathode of the photomultiplier tube and also affect photocathode efficiency²⁶. Photomultiplier noise is low in amplitude and usually eliminated by discriminator circuits.

When a scintillator detector is placed in operation, it is important to ensure that the photomultiplier tube voltage, amplifier gain and discriminator settings are adjusted so that the radiation of interest produces pulses which the electronic circuits are capable of handling. If some pulses are excessively large, amplifier circuits tend to block for a time after each excessive pulse and hence cause a prolongation of the dead time of the instrument.

In the light of above observations, it leads to a conclusion that to design a portable dose rate meter with an NE102A plastic scintillator will be useful exercise.

References

1. C.D.Zerby and H.S.Moran, Nucl.Inst.Meth. 14(1961)115.
2. R.J.D.Beatie and Byrane, Nucl.Inst.Meth.104(1972)164.
3. B.Grosswendt and Waibel, Nucl.Inst.Meth.131(1975)143.
4. B.F.Peterman, S.Hontzeas and R.G.Rystephanik,
Nucl.Inst.Meth.104(1972)461-468.
5. B.Lal and K.V.K.Iyengar, Nucl.Inst.Meth. 79(1970)19.
6. E.Nardi, Nucl.Inst.Meth. 95(1971)229.
7. N.A.Lurie, L.Harris.Jr, and J.C.Young
Nucl.Inst.Meth. 129(1975)843.
8. O.Klein and Y.Nishina, Z.Physik, 52 (1929)853.
- 9 R.D.Evans, "x-ray and γ -ray interactions" in Radiation Dosimetry, Vol.1.F.H.Attix, and W.C.Roesch,eds.pp~99 Academic Press, N.Y.(1968).
10. A.E.Profio, Radiation Shielding and Dosimetry, p-74 Wiley, N.Y.(1979)
11. International Commission on Radiation Units and Measurements,ICRU Report 19, Radiation Quantities and Units (International Commission on Radiation Units and Measurements, Washington, D.C. 1975)
12. E.Storm and H.I.Israel, Nucl.Data.Table A7(1970)565.
13. J.H.Hubbell,Nat.Stand.Ref.Data.Ser.NSRDS-NBS 29(1969)
14. C.D.Zerby , Meth.Comp.Phys. 1(1963)89.
15. F.H.Attix, Phys. Med. Biol. 13(1968)119.
16. J.H.Hubbel Radiat. Res. 58(1977)70.
17. Nuclear Enterprises Detector brochure number 126P,
February,1980.

18. ICRU Report 21, Radiation Dosimetry: Electrons with initial energies between 1 and 50 MeV. International Commission on radiation Units and Measurements.

Washington, D.C.(1974).

19. F.W.Spiers, M.J.McHugh and D.B.Appleby, "The Natural Radiation Environment"(J.A.S.Adams and W.M.Lowder eds) pp-885.Univ.of Chicago Press,Chicago, Illinois(1964).

20. G.P.Hanson and E.Komarov, "Proceeding of a Symposium on biological effect of low level radiation" IAEA-SM-266-81 pp-211 (1983),Vienna.

21. United Nations Scientific Committee on the Effects of Atomic Radiation, Sources and effects of Ionizing radiation, 1977 Report to General Assembly, with Annexes, UN, N.Y.(1977).

22. J.Boag, "Ionization Chambers" in Radiation, Dosimetry, Vol. 2.F.H.Attix, and W.C.Roesch,eds.pp-2 Academic Press,New,York(1966).

23 W.V.Mayneord and C.R.Hill, "Natural and man-made background radiation" in Radiation Dosimetry, Vol. 3.F.H.Attix, and W.C.Roesch,eds.pp-426 Academic Press,New,York(1966).

24. A.H.Smith, S.Clarks and G.W.Reed,
Int.J.Appl.Radiat.Isotopes 18(1967)647.

25. T.A.Iinuma and P.R.J.Burch, Nucl.Inst.Meth.16(1962)247.

26. ICRU Report 20, Radiation Protection Instruments and its application. International Commission on Radiation Units and Measurements, Washington, D.C., (1976)

APPENDIX

(Listing of Computer programs.)

MONTE CARLO ROUTINE TO DETERMINE THE ENERGY RESPONSE SPECTRUM
OF NE102A PLASTIC SCINTILLATOR.

C EP PHOTON ENERGY IN CROSS-SECTION TABLE
 C SPRPE.....PROBABILTY OF PHOTOEFFECT IN SCINTLLATOR
 C SPRC " COMPTON
 C SPRP " PAIR " "
 C NIP NUMBER OF INITIAL PHOTON
 C EK TOTAL ELECTRON ENERGY AT THE END OF COLLISION
 C R RANDOM NUMBER
 C E INITIAL ENERGY OF PHOTON
 C E0 E/.511006
 C R0 CLASSICAL ELECTRON RADIUS
 C PSCSCO....SCINTILATOR COMPTON CROSS-SECTION(KLEIN-NISHINA)
 C F DIFFERENTIAL " " (")
 C S F/PSCSCO (RANDOM NUMBER)
 C E1 SCATTERED PHOTON ENERGY
 C ECE ELECTRON ENERGY
 C MUT ATTENUATION COEFFICIENT
 C RADI RADIUS OF SCINTILLATOR
 C THIK THICKNESS OF SCINTILLATOR
 C EPEP ELECTRON ENERGY IN PHOTOEFFECT
 C EKT TOTAL ELECTRON KINETIC ENERGY
 C CPCNL.....COUNTS PER CHANNEL
 C K CHANNEL NUMBER
 C PE1.....FIRST INTERACTION ABSORPTION
 C PE2.....SECOND ABSORPTION

```

PROGRAM MONCA(INPUT,TAPE4,TAPE6=INPUT,OUTPUT)
COMMON EP(30),SPRPE(30),SPRC(30),SPRP(30),PMU(30)
COMMON/INIT/ X0,Y0,Z0,COSALPO,COSBET0,COSGAM0
COMMON/SPEC/ NG,DIS1,PMUT,EK,RADI,THIK
COMMON/FLG/ PRFLAG
COMMON/COUNT/ CPCNL(1330)
DO101 I=1,30
READ(4,*)EP(I),SPRPE(I),SPRC(I),SPRP(I),PMU(I)
PRINT*,EP(I),SPRPE(I),SPRC(I),SPRP(I),PMU(I)
CONTINUE
CPCNL(K)=0
PE1=0
PE2=0
READ(6,*)NIP,E7,RADI,THIK
READ(6,*)NIP,RADI,THIK
PRINT*,NIP,E7,RADI,THIK
NPID=0

```

101

C..

C..... THE RANSET SUBROUTINE CALL, INITIALIZES THE SEED OF INTRINSIC
 C..... FUNCTION RANF, TO GENERATE RANDOM NUMBER
 C.....

```

CALL RANSET(2)
DO 500,NG=1,NIP
C PRINT503/NG
503 FORMAT(3X,11HPHOTON NO=',I5)
CALL COB(E7)
E=E7
C PRINT*,E
EK=0
FRFLAG=0
X0=0.0
Y0=0.0
Z0=0.0
COSALP0=0.0
COSBET0=0.0
COSGAM0=1.0
DO125 I=1,30
IF(E.LE.EP(I))GOTO126
CONTINUE
126 PMUT=PMU(I)-(PMU(I)-PMU(I-1))*(EP(I)-E)/(EP(I)-EP(I-1))
PX=EXP(-PMUT*THIK)
R=RANF()
R=R*(1.-PX)
DIS1 =- ALOG(1.-R)/PMUT
C PRINT222,PMUT,THIK,1.-PX,R,ALOG(R),DIS1
222 FORMAT(2X,6(E12.4))
IF(DIS1.GT.THIK)GOTO 500
NPID=NPID+1
CALL PROB(E,PRPE,PRC,PRP)
R=RANF()
IF(R.LE.PRPE)THEN
CALL PHOTO(E,PE3,PE1)
ELSE IF(R.LE.(PRP+PRPE))THEN
CALL PAIR(E,G)
ELSE
CALL COMP(E,E1,PE4,PE2)
ENDIF
500 CONTINUE
PRINT*,NIP,NPID
PRINT765,PE1
765 FORMAT(2X,'FIRST INTR ABS=',E12.4)
PRINT785,PE2
785 FORMAT(2X,'COMPT INTR ABS=',E12.4)
C..
C.. FINAL RESULTS
DO 1002 K=1,1330
  
```

```

IF(CPCNL(K).LE.0.0)GOTO 1001
PRINT700,K,CPCNL(K)
1001 CONTINUE
700  FORMAT(10X,I4,8X,E12.5)
1002 CONTINUE
STOP
END

```

C

```

SUBROUTINE COB(E7)
ECO1=1.33
ECO2=1.17
PCO1=.50
PCO2=.50
R=RANF()
IF(R.LE.PCO1)THEN
E7=ECO1
ELSE
E7=ECO2
ENDIF
RETURN
END

```

C..

```

SUBROUTINE PROB(E,PRPE,PRC,PRP)
COMMON EP(30),SPRPE(30),SPRC(30),SPRP(30),PMU(30)
COMMON/SPEC/ NG,DIS1,PMUT,EK,RADI,THIK
DO103,I=1,30
IF(E.LE.EP(I))GOTO 104
103 CONTINUE
104 PLPE=SPRPE(I)-(SPRPE(I)-SPRPE(I-1))*((EP(I)-E)/(EP(I)-EP(I-1)))
PLC=SPRC(I)-(SPRC(I)-SPRC(I-1))*((EP(I)-E)/(EP(I)-EP(I-1)))
PLP=SPRP(I)-(SPRP(I)-SPRP(I-1))*((EP(I)-E)/(EP(I)-EP(I-1)))
PRPE=PLPE
PRC=PLC
PRP=PLP

```

C

```
PRINT9,E,EP(I),SPRPE(I),SPRC(I),SPRP(I),PRPE,PRC,PRP

```

C9

```
FORMAT(10(1X,E12.3))

```

C9

```
FORMAT(2X,'E=',E12.4,2X,'E5=',E12.4,2X,'RE=',E12.4,2X,

```

C

```
'RC=',E12.4,2X,'RP=',E12.4)

```

```
RETURN
END

```

C..

```
SUBROUTINE PHOTO(E,PE3,PE1)

```

```
COMMON/COUNT/ CPCNL(1330)

```

```
COMMON/SPEC/ NG,DIS1,PMUT,EK,RADI,THIK

```

C..

```
PE1=1+PE1

```

```
EKT=E

```

```
K=INT(1000*EKT)

```

```

CPCNL(K)=CPCNL(K)+1
RETURN
END

C...
SUBROUTINE PAIR(E,G)
COMMON/INIT/ X0,Y0,Z0,COSALPO,COSBETO,COSGAM0
COMMON/SPEC/ NG,DIS1,PMUT,EK,RADI,THIK
COMMON/FLG/ PRFLAG
COMMON/COUNT/ CPCNL(1330)
EXPE=THE KINETIC ENERGY OF THE CREATED POSITRON-ELECRON PAIR
EEPP=ELECTRON ENERGY IN PAIR PRODUCTION
EPHMX=PHOTON ENERGY, AFTER ANNIHILATION OF THE POSITRON.

C.. IF(E.LT.1.022)RETURN
C.. EXPE=(E-1.022)
C.. PRFLAG=1
C.. EEPP=EXPE/2
C.. K=INT(1000*EEPP)
C.. CPCNL(K)=CPCNL(K)+1
C.. IF(PRFLAG.EQ.1)CPCNL(K)=CPCNL(K)+1
C.. EPHMX=0.511006
C.. E=0.511006
C.. CALL COMP(E,E1,PE4,PE2)
C.. RETURN
C.. END

C...
SUBROUTINE COMP(E,E1,PE4,PE2)
COMMON EP(30),SPRPE(30),SPRC(30),SPRP(30),PMU(30)
COMMON/INIT/ X0,Y0,Z0,COSALPO,COSBETO,COSGAM0
COMMON/SPEC/ NG,DIS1,PMUT,EK,RADI,THIK
COMMON/FLG/ PRFLAG
DIMENSION S(18),T(18)
COMMON/COUNT/ CPCNL(1330)

C.. NCI=NO.OF COMPTON INTERACTION
C.. NCI=1
C.. R0=2.818 E-13
C.. A=3.141592654*R0**2
C.... THE FOLLOWING EQN. IS KLEIN-NISHINA FORMULA
C304 PSCSCO=2.*3.141592654*R0**2*((2.*E0**4+18.*E0**3+
C.. + 16.*E0**2+4.*E0+(1.+2.*E0)**2*(E0**2-2.*(1.+E0))
C.. + * ALOG(1.+2.*E0))/2.*E0**3*(1.+2.*E0)**2)
C.....
304 E0=E/.511006
P1=2.*A
P2=(4.*E0+16.*E0**2+18.*E0**3+2.*E0**4)
P3=(1.+2.*E0)**2*(E0**2-2.*(1.+E0))*ALOG(1.+2.*E0)
P4=2.*E0**3*(1.+2.*E0)**2

```

```

P5=P2+P3
PSCSCO=P1*P5/P4
B=4.+10.*E0+8.*E0**2+E0**3
C.... FROM HERE TO TETA=T1, WE CALCULATE TETA TO DETERMINE SCATTERED
C.... PHOTON ENERGY.
R=RANF()
DO305 I=1,18
T(I)=(1.74532925E-01)*I
COST=COS(T(I))
C B=4.+10.*E0+8.*E0**2+E0**3
C C=(4.+16.*E0+16.*E0**2+2.*E0**3)*COST
D=(6.*E0+10.*E0**2+E0**3)*(COST)**2 - 2.*E0**2*(COST)**3
V=2.*E0**2*(1.+E0*(1.-COST))**2
U0=((E0**2-2.*(1.+E0))* ALOG(1.+E0*(1.-COST)))/E0**3
F=A*(U0+(B - C + D)/V)
S(I)=F/PSCSCO
IF(R.LE.S(1))GOTO5201
IF(R.LE.S(I))GOTO 5001
CONTINUE
305
C..
C DO306 N=1,17
C IF(R.LE.S(1))GOTO5201
C IF(R.LE.S(N+1))GOTO 5001
C306
C.. CONTINUE
5201 DO1110 L=1,100
T1=(1.74532925E-03)*L
COST1=COS(T1)
C B1=4.+10.*E0+8.*E0**2+E0**3
C C1=(4.+16.*E0+16.*E0**2+2.*E0**3)*COST1
D1=(6.*E0+10.*E0**2+E0**3)*(COST1)**2 - 2.*E0**2*(COST1)**3
V1=2.*E0**2*(1.+E0*(1.-COST1))**2
U1=((E0**2-2.*(1.+E0))* ALOG(1.+E0*(1.-COST1)))/E0**3
F1=A*(U1+(B - C1 + D1)/V1)
S1=F1/PSCSCO
IF(R.LE.S1)GOTO 5011
1110
CONTINUE
5001
TE=T(I-1)
TE=T(N)
DO1010 L=1,100
T1=TE+(1.74532925E-03)*L
COST1=COS(T1)
C B1=4.+10.*E0+8.*E0**2+E0**3
C C1=(4.+16.*E0+16.*E0**2+2.*E0**3)*COST1
D1=(6.*E0+10.*E0**2+E0**3)*(COST1)**2 - 2.*E0**2*(COST1)**3
V1=2.*E0**2*(1.+E0*(1.-COST1))**2
U1=((E0**2-2.*(1.+E0))* ALOG(1.+E0*(1.-COST1)))/E0**3
F1=A*(U1+(B - C1 + D1)/V1)
C5001

```

```

S1=F1/PSCSCO
IF(R.LE.S1)GOTO 5011
CONTINUE
1010 TETA=T1
5011 COSTETA=COS(TETA)
C..
IF(NCI.GT.1)GOTO807
X1 =X0+DIS1*COSALP0
Y1 =Y0+DIS1*COSBETO
Z1 =Z0+DIS1*COSGAM0
U =SQRT(X1**2+Y1**2)

HERE CALCULATE SCATTERED PHOTON ENERGY.
C.. 807 E1=E/(1.+E0*(1.-COSTETA))
      ECE=E-E1
      EK=EK+ECE
      PRINT909,X1,Y1,Z1,COSALP0,COSBETO,COSGAM0,TETA ,DIS1,PMUT,E1,EK
      FORMAT(11(E12.3))

C.. 909 C..
      R=RANF()
      PHI=2.*3.141592654*R
      TRANSFORMATION OF SCATTERING ANGLE INTO REFERENCE CYLINDER
      SINTETA=SIN(TETA)
      SINPHI =SIN(PHI)
      COSPHI =COS(PHI)
      ACZ=ABS(COSGAM0)

C..
      IF(ACZ.GE.1.0)GOTO808
      SQ1=(1.- (COSGAM0)**2)
      SQ2=SINTETA/SQRT(SQ1)
      COSALP1=COSTETA*COSALP0 + SQ2*
      + (COSALP0*COSGAM0*COSPHI - COSBETO*SINPHI)
      COSBET1=COSTETA*COSBETO + SQ2
      + *(COSBETO*COSGAM0*COSPHI + COSALP0*SINPHI)
      COSGAM1=COSTETA*COSGAM0 - SQ2*SQ1*COSPHI
      GOTO809

C.. 808 C..
      COSALP1=SINTETA*COSPHI
      COSBET1=SINTETA*SINPHI
      COSGAM1=(COSGAM0/ACZ)*COSTETA
      E=E1
      CALL PROB(E,PRPE,PRC,PRP)
      R=RANF()

C.. 907 PRINT907,E,PRPE,PRC,PRP,R
      FORMAT(11X,E12.3))
      IF(R.LE.PRPE)GOTO 4040
      IF(R.LE.(PRPE+PRP))GOTO 5022
      DO125 I=1,30

```

```

125 IF(E.LE.EP(I))GOTO126
126 CONTINUE
PMUT=PMU(I)-(PMU(I)-PMU(I-1))*(EP(I)-E)/(EP(I)-EP(I-1))
R=RANF()
DIS1 =- ALOG(R)/PMUT
X0=X1
Y0=Y1
Z0=Z1
COSALP0=COSALP1
COSBETO=COSBET1
COSGAM0=COSGAM1
X1 =X0+DIS1*COSALP0
Y1 =Y0+DIS1*COSBETO
Z1 =Z0+DIS1*COSGAM0
U =SQRT(X1**2+Y1**2)
IF(U .GT.RADI)GOTO501
IF(Z1.GT.THIK)GOTO501
IF(Z1.LE.0.0 )GOTO501
NCI=NCI+1
GOTO 304
C..
C.. PHOTON-ABSORPTION
4040 EKT=E+EK
K=INT(1000*EKT)
CPCNL(K)=CPCNL(K)+1
PE2=1+PE2
RETURN
C..
C.. PAIR PRODUCTION
C EXPE=THE KINETIC ENERGY OF THE CREATED POSITRON-ELECTRON PAIR
C EEPP=ELECTRON ENERGY IN PAIR PRODUCTION
C EPHMX=THE PHOTON ENERGY, AFTER ANNIHILATION OF THE POSITRON.
5022 IF(E1.LT.1.022)GOTO501
EXPE=(E1-1.022)
PRFLAG=1
EEPP=EXPE/2
K=INT(1000*EEPP)
CPCNL(K)=CPCNL(K)+1
IF(PRFLAG.EQ.1)CPCNL(K)=CPCNL(K)+1
EPHMX=0.511006
E=EPHMX
GOTO 304
C..
501 IF(EK.LT..001)EK=.001
K=INT(1000*EK)
IF(K.GE.500)PRINT*,NG
CPCNL(K)=CPCNL(K)+1
RETURN

```

99

END

PROGRAM DOSE(INPUT,TAPE3,TAPE4,TAPE5,TAPE6,OUTPUT)

C
C....THIS PROGRAM CALCULATE THE DOSE PER PHOTON FROM MONTE CARLO
C....SPECTRUM AND FROM SPECIFIC GAMMA RAY CONSTATNT,
C....AND ALSO CALCULATE THE RESPONSE OF NE102A RELATIVE
C....TO MUSCLE.
C....1.602E-8=CONVERT MEV/GM TO RAD AND/.877 CONVERTS RAD TO RONG
C....PHOTON FLUX PER ROENGEN=5.475E+7/E*(MUEN/RHO)AIR PH/CM**2-R
C....ROENGEN/HR=5.475E+7/3.6E+3*E*(MUEN/RHO)AIR PH/CM**2-SEC
C....1/4PHI(100)**2=7.9577471E-6
C....AREA=PI*RADIUS**2= 1 CM**2
C....EP=ENERGY OF PHOTON IN PROB. TABLE FOR PLASTIC
C....PRPE=PROBABILITY FOR PHOTO-EFFECT
C....PRC=PROBABILITY FOR THE COMPTON EFFECT
C....PRP=PROBABILITY FOR PAIR PRODUCTION
C....PMUT=TOTAL CROSS SECTION OF NE102A
C....ARMS=MASS ENERGY ABSORPTION CO-EFFICIENT OF AIR
C....ARPL=RATIO (AIR/PLASTIC) OF MASS-ENERGY ABSORPTION COEFFICIENT
C....ARMM=RATIO (AIR/TISSUE) OF MASS-ENERGY ABSORPTION COEFFICIENT
C....E=ENERGY IN MONTE CARLO SPECTRUM FOR PLASTIC
C....CPCNL=COUNT PER CHANNEL,...SET=ENERGY IN MEV
C....ES=ENERGY OF PHOTON IN TISSUE PROB. TABLE
C....TSPE=PROBABILITY FOR PHOTO-EFFECT IN TISSUE
C....TSC=PROBABILITY FOR THE COMPTON EFFECT
C....TSP=PROBABILITY FOR PAIR PRODUCTION
C....TSMUT=TOTAL CROSS SECTION OF TISSUE
C....V=ENERGY IN MONTE CARLO SPECTRUM FOR TISSUE
C....TSCNL=COUNTS PER CHANNEL(TISSUE SPECTRUM)
C....TSET=ENERGY IN MEV
C....H=THICKNESS OF DETECTOR
C....E2=INCIDENT ENERGY
C....NDP=NO.OF DATA POINT IN SPECTRUM
C....PNI=(1-EXP(-XMU)) FOR PLASTIC
C....TSNI=(1-EXP(-XMU)) FOR TISSUE
C....1E+4=10000 INTERACTED PHOTON IN PLASTIC
C....TAU=SPECIFIC GAMMA RAY CONST.
C....CIHR=CURIE PER HOUR
C....DMS=DETECTOR MASS
C....DOSK=ENERGY PER GRAM PER PHOTON
C....DOSP=DOSE/PHOTON IN ROENTGEN
C....DOSS=TOTAL DOSE IN ROENTGEN
C....RPPH=ROENTGEN/PHOTON FROM GAMMA CONST.
C....RPPHM=ROENTGEN/PHOTON FROM MONTE CARLO (PLASTIC)
C....RTSHM=ROENTGEN/PHOTON FROM MONTE CARLO (TISSUE)
C....RMED=AIR-MEDIUM ABSORPTION RATIO
C.....
C

COMMON/PLA/ EP(30),PRPE(30),PRC(30),PRP(30),PMUT(30)
 COMMON/RPL/ ARMS(30),ARPL(30)
 COMMON/RTS/ARMM(22),ARTS(22)
 COMMON/PLMEN/ E(1000),CPCNL(1000),SET(1000)
 COMMON/TIS/ ES(22),TSPE(22),TSC(22),TSP(22),TSMUT(22)
 COMMON/TMSL/ V(1000),TSCNL(1000),TSET(1000)
 COMMON H,E2,NDP

C

H=5.080

E2=1.00

DO700 I=1,30

700 READ(3,*)EP(I),PRPE(I),PRC(I),PRP(I),PMUT(I),ARMS(I),ARPL(I)

CONTINUE

IF(E2.EQ.1.00)NDP=1000

DO10 K=1,NDP

READ(4,*)E(K),CPCNL(K)

10 CONTINUE

DO705 K=1,22

705 READ(5,*)ES(K),TSPE(K),TSC(K),TSP(K),TSMUT(K),ARTS(K),ARMM(K)

CONTINUE

DO15 K=1,NDP

READ(6,*)V(K),TSCNL(K)

15 CONTINUE

CALL PLDOS(PNI,RPPHM)

CALL TSDOS(TSNI,RTSHM)

C.... PLTS=RATIO (PLASTIC/TISSUE) OF ENERGY ABSORBED (ROENTGEN/PHOTON)

PLTS=RPPHM/RTSHM

SMI=1E+4*TSNI/PNI

PRINT555,SMI

555 FORMAT(2X,'PHOTON TO BE INTERACTED IN TSO=',E12.6)

PRINT1111,PLTS

1111 FORMAT(2X,'PLSTK/MUSCL=',E12.3)

STOP

END

C.....

C

SUBROUTINE PLDOS(PNI,RPPHM)

COMMON/PLA/ EP(30),PRPE(30),PRC(30),PRP(30),PMUT(30)

COMMON/RPL/ ARMS(30),ARPL(30)

COMMON/PLMEN/ E(1000),CPCNL(1000),SET(1000)

COMMON H,E2,NDP

PRINT400

400 FORMAT(2X,6HPLASTK)

PRINT500,H,E2

500 FORMAT(2X,'THIKNESS CM=',E12.4,3X,'ENERGY IN MEV =',E12.4)

RHO=1.032

DMS=RHO*H

SETJ=0

```

CPCNLK=0
DO1000 J=1,NDP
IF(CPCNL(J).EQ.0)GOTO1000
SET(J)=(E(J)/1000)*CPCNL(J)
1000 CONTINUE
DO300 J=1,NDP
SETJ=SETJ+SET(J)
CPCNLK=CPCNLK + CPCNL(J)
300 CONTINUE
PRINT350,CPCNLK,SETJ
350 FORMAT(2X,'PHOTN INTRK=',E12.6,3X,'ENERGY IN SPKTRM=',E12.4)
SNDT=SETJ
TPI=CPCNLK
DO 250 J=1,30
IF(E2.LE.EP(J))GOTO450
250 CONTINUE
450 PMU=PMUT(J)-(PMUT(J)-PMUT(J-1))*((EP(J)-E2)/(EP(J)-EP(J-1)))
C PRINT*,PMU
XMU=PMU*H
PNI=1-EXP(-XMU)
C...
NIP=NO.OF PHOTON INCIDENT
NIP=TPI/PNI
ENCON=SETJ/(NIP*E2)
PRINT600,NIP,ENCON
600 FORMAT(2X,'PHOTN INCDNT=',I7,2X,'PROP CONST.K=',E12.3)
DOSK=SNDT/(DMS*NIP)
DO 402 J=1,30
IF(E2.LE.EP(J))GOTO403
402 CONTINUE
403 RMED=ARPL(J)-(ARPL(J)-ARPL(J-1))*((EP(J)-E2)/(EP(J)-EP(J-1)))
PRINT888,RMED
888 FORMAT(2X,'MUENR AIMED RATIO=',E12.4)
DOSP=(1.602E-8)/.877*DOSK*RMED
DO 404 J=1,30
IF(E2.LE.EP(J))GOTO405
404 CONTINUE
405 ARMU=ARMS(J)-(ARMS(J)-ARMS(J-1))*((EP(J)-E2)/(EP(J)-EP(J-1)))
C PRINT*,ARMU
DOSS=DOSP*NIP
TAU=19.4*E2*ARMU
CIHR=1.332E+14
RPPH=TAU/CIHR
RPPHM=DOSP*7.9577471E-6
PRINT110,DOSK,DOSP
PRINT200,DOSS,TAU
PRINT555,RPPH,RPPHM
110 FORMAT(2X,'ENRG/GM/PTN=',E12.4,3X,'DOSE/PTN IN RON =',E12.4)
200 FORMAT(2X,'DOSTOT(RON)=',E12.4,3X,'GAMA RAY CONSTNT=',E12.4)

```

```

555  FORMAT(2X,'GAMA DOSRAT=',E12.4,3X,'DOSRATE MONTKRLO=',E12.4)
      RATIO=RPPH/RPPHM
      PRINT9000,RATIO
9000  FORMAT(2X,'GAMMA DOSE RATIO FOR PLASTIC=',E12.6)
      RETURN
      END
C.....
C
      SUBROUTINE TSDOS(TSNI,RTSHM)
      COMMON/TIS/ ES(22),TSPE(22),TSC(22),TSP(22),TSMUT(22)
      COMMON/RTS/ ARMM(22),ARTS(22)
      COMMON/TMSL/ V(1000),TSCNL(1000),TSET(1000)
      COMMON H,E2,NDP
      PRINT400
400   FORMAT(2X,6HT ISSUE)
      RHO=1.000
      PRINT500,H,E2
500   FORMAT(2X,'THIKNESS CM=',E12.4,3X,'ENERGY IN MEV     =',E12.4)
      TSETJ=0
      TSCNLK=0
      DO1000 J=1,NDP
      IF(TSCNL(J).EQ.0)GOTO1000
      TSET(J)=(V(J)/1000)*TSCNL(J)
1000   CONTINUE
      DO300 J=1,NDP
      TSETJ=TSETJ+TSET(J)
      TSCNLK=TSCNLK + TSCNL(J)
300   CONTINUE
      PRINT350,TSCNLK,TSETJ
350   FORMAT(2X,'PHOTN INTRK=',E12.6,3X,'ENERGY IN SPKTRM=',E12.4)
      TSDT=TSETJ
      TSI=TSCNLK
      DO 250 J=1,22
      IF(E2.LE.ES(J))GOTO450
250   CONTINUE
450   TSMU=TSMUT(J)-(TSMUT(J)-TSMUT(J-1))*((ES(J)-E2)/(ES(J)-ES(J-1)))
      PRINT*,TSMU
      DMS=RHO*H
      XMU=TSMU*H
      TSNI=1-EXP(-XMU)
      NIP=TSI/TSNI
      PRINT600,NIP
600   FORMAT(2X,'PHOTN INCDNT=',I7)
      DOSK=TSDT/(DMS*NIP)
      DO 402 J=1,22
      IF(E2.LE.ES(J))GOTO403
402   CONTINUE
403   RMED=ARMM(J)-(ARMM(J)-ARMM(J-1))*((ES(J)-E2)/(ES(J)-ES(J-1)))

```

```
PRINT888,RMED
888  FORMAT(2X,'MUENR AIRMED RATIO=',E12.4)
      DOSP=(1.602E-8)/.877*DOSK*RMED
      DO 404 J=1,22
      IF(E2.LE.ES(J))GOTO405
404  CONTINUE
405  C
      ARMU=ARTS(J)-(ARTS(J)-ARTS(J-1))*((ES(J)-E2)/(ES(J)-ES(J-1)))
      PRINT*,ARMU
      DOSS=DOSP*NIP
      TAU=19.4*E2*ARMU
      CIHR=1.332E+14
      RPPH=TAU/CIHR
      RTSHM=DOSP*7.9577471E-6
      PMICRH=0.015208/(E2*ARMU)
      PRINT110,DOSK,DOSP
      PRINT200,DOSS,TAU
      PRINT555,RPPH,RTSHM
110  FORMAT(2X,'ENRG/GM/PTN=',E12.4,3X,'DOSE/PTN IN RON =',E12.4)
200  FORMAT(2X,'DOSTOT(RON)=',E12.4,3X,'GAMA RAY CONSTNT=',E12.4)
555  FORMAT(2X,'GAMA DOSRAT=',E12.4,3X,'DOSRATE MONTKRLO=',E12.4)
      RATIO=RPPH/RTSHM
      PRINT9000,RATIO
9000 FORMAT(2X,'GAMMA DOSE RATIO FOR TISSUE=',E12.6)
      RETURN
      END
```

PROGRAM SMEAR(INPUT,TAPES=INPUT,OUTPUT)

C
C... THE SMEARING OUT OF THE MONTE CARLO RESULTS IS DONE
C... BY THIS PROGRAM "SMEAR".
C... C(N)=NO.OF COUNTS IN N'TH CHANNEL
C... SIGMA= FWHM/2.35482
C... GAUSSIAN DISTRIBUTION IS F(I)
C... F(I)=[C(N)/SIGMA*SQRT 2P] EXP0-(I-N)**2/2*SIGMA**2
C... S(M)=NO.OF COUNTS IN SMEARED SPECTRUM
C
DIMENSION F(1000),C(1000),S(1000)
C
DO 100 I=1,266
READ(5,*)C(I)
CONTINUE
FW=30
SIGMA=FW/2.35482
DN=SQRT(2*3.1415926)*SIGMA
DN2=2*SIGMA**2
DO105 K=1,252
N=15+K-1
DO 101 J=1,30
F(J)=(C(N)/DN)*EXP(-(J+K-2-N)**2/DN2)
PRINT103,J,C(N),F(J)
CONTINUE
DO106 L=1,30
M=L+K-1
S(M)=S(M)+F(L)
CONTINUE
CONTINUE
DO108 M=1,300
PRINT103,M,S(M)
CONTINUE
FORMAT(2X,I4,3X,E12.4)
STOP
END

PROGRAM BKGRND(INPUT,TAPE4=INPUT,OUTPUT)

```

C
C....NC=NO.OF CHANNEL,.....CPCNL=NO.OF COUNTS IN CHANNEL
C....TCN=TOTAL NO. OF COUNTS,.....AVEC=AVERAGE COUNTS
C....RSP=RESPONSE,.....H=THICKNESS,.....RDUS=RADIUS
C....DMS=DETECTOR MASS
C....BKGPS=BACKGROUND PER SEC IN MEV
C....BGRPS=          "          MICRORAD
C....BGRDH=          "          HOUR
C....BGMRNH=          "          MICROROENTGEN
C....BGGYH=          "          MICROGRAY
C....BGGY=          "          YEAR    MILIGRAY
C.....
C
DIMENSION X(1020),CPNL(1020)
PRINT*, 'DATE 7 8 1 PM'
CPNLK=0
TCN=0
NC=499
TIM=1000
PRINT500,TIM
500 FORMAT(6X,'TIME IN SECOND=',E12.4)
DO 100 I=1,NC
C
READ(4,*)X(I),CPNL(I)
READ(4,*)CPNL(I)
100 CONTINUE
DO 900 K=1,NC
TCN=TCN+CPNL(K)
AVEC=TCN/NC
900 CONTINUE
PRINT505,TCN ,AVEC
505 FORMAT(/,6X,'TOTAL COUNT=',E12.4,2X,'AVERAGE=',E12.4)
DO300 J=1,NC
IF(J.LE.10)RSP=.851
IF(J.GT.10.AND.J.LE.20)RSP=.858
IF(J.GT.20.AND.J.LE.40)RSP=.869
IF(J.GT.40)RSP=.983
ENC=6.1
CPNL(J)=ENC*J*CPNL(J)/RSP
300 CONTINUE
DO200 K=1,NC
CPNLK=CPNLK+CPNL(K)
200 CONTINUE
H=5.08
RDUS=2.54
RHO=1.032
PI=3.141592654

```

```
DMS=PI*RHO#H*RDUS*RDUS
TC=CPNLK
BKGPS=TC/(TIM*DMS)
BGRPS=1.602E-11*BKGPS
BGRDH=3600*BGRPS*1E+06
BGMRNH=BGRDH/.877
BGGYH=BGRDH*1E-02
BGGY=24*365*BGGYH*1E-03
PRINT105,BKGPS,BGRPS
PRINT107,BGRDH,BGMRNH
PRINT106,BGGYH,BGGY
105 FORMAT(/,6X,'BG(KEV)/SEC=',E12.4,2X,'BGRAD/SEC=',E12.4)
107 FORMAT(/,6X,'MICRAD/HR=',E12.4,2X,'MICRON/HR=',E12.4)
106 FORMAT(/,6X,'BG MICGY/HR=',E12.4,2X,'BGMLGY/YR=',E12.4)
STOP
END
```